

ELECTROMAGNETIC SCATTERING PROPERTIES  
OF A RESONANT PLASMA

Thesis by  
Haskell Shapiro

In Partial Fulfillment of the Requirements  
for the Degree of  
Doctor of Philosophy

California Institute of Technology  
Pasadena, California

1957

## ACKNOWLEDGEMENTS

The writer wishes to express his indebtedness to his advisor, Dr. C. H. Papas, for his helpful guidance and encouragement throughout the course of this research.

Sincere thanks are due to those who provided assistance to the writer in fabrication of the experimental apparatus, recording the experimental results, and preparation of the manuscript.

## ABSTRACT

A column of ionized mercury vapor is placed in a parallel plate transmission line and the resulting reflection coefficient observed. From the measurement of reflection coefficient as a function of discharge current, plasma resonance is demonstrated. In accordance with the theory applied, but in contrast to the results of other investigators, resonance is found at only one value of discharge current. The discharge current required to produce resonance is measured as a function of frequency. The functional dependence observed is as predicted by theory, but the current is higher than the theoretical value. The discharge current required to produce resonance is measured as a function of gas pressure. The dependence that is found follows that predicted theoretically at higher gas pressures, but deviates sharply from the theoretical form at lower gas pressures.

## TABLE OF CONTENTS

I	INTRODUCTION	1
II	THEORETICAL RELATIONS	3
	A. Nomenclature	3
	B. Dielectric Properties of a Plasma	7
	C. The Equations Governing Scattering	9
	D. Scattering by a Homogeneous Dielectric Cylinder	11
	E. Scattering by a Thin Cylinder	13
	F. Quasi-Static-Resonances of Other Shapes	15
	G. Gaseous Discharge Tube in a Parallel Plate Line	18
	1. The Idealized Case	18
	2. Effect of Quasi-Static Approximation	22
	3. Effect of Non-Uniform Plasma Density	24
	4. Effect of Finite Cylinder Radius	27
	5. Effect of Finite Tubing Thickness	34
	6. Effect of Finite Line Width	36
	H. Properties of a Gaseous Discharge	38
	J. Summary of Theoretical Relations	41
III	EXPERIMENTAL APPARATUS AND TECHNIQUES	43
	A. Choice of Experimental Method	43
	B. Description of Apparatus	46
	C. Calibration and Operating Technique	48
IV	RESULTS AND DISCUSSION	51
V	FIGURES	53
VI	LIST OF REFERENCES	63

## I INTRODUCTION

The discovery and utilization of scatter propagation (1) has led to interest in the details of the mechanism of this mode of "beyond-the-horizon" radio transmission. Some investigators (2,3) have examined the possibility that the ionized trails from meteors may play an important part in this mode of propagation. It is well known (4) that strong radio echoes may be obtained from meteor trails.

It has been pointed out by Herlofson (2) that under certain conditions a resonance effect may exist in the scattering of a plane wave by an ionized cylinder. When this resonance effect occurs, the effective scattering diameter of the cylinder may be many times greater than its physical diameter. The presence of this enhanced effectiveness of scattering may be correlated with the excitation of "plasma resonance", an effect apparently first described by Eckersley (5).

The phenomenon of "plasma resonance" involves the existence of a frequency at which a particular configuration of an ionized gas will be strongly excited by an externally generated electric field. The frequency at which this occurs, called the critical frequency by Herlofson, depends on both the shape of the plasma and which of its possible modes is excited. This frequency is distinct from the "plasma frequency" familiar to workers in the field of gaseous discharges. However, for certain shapes, the frequencies may assume the same value.

Only a few investigators have done experimental work in the field of plasma resonance. In 1931 Tonks (6,7) reported a series of experiments in which he placed a discharge tube between the plates of a parallel plate capacitor. He verified the existence of plasma resonance, and the dependence of the phenomenon on the shape of the plasma. However,

his method did not permit a quantitative evaluation of the effect of the presence of the plasma on the terminal impedance of the parallel plate capacitor. Tonks observed changes in the impedance of the capacitor at discharge tube currents other than that at which plasma resonance was expected to occur. In 1951 Romell (8) reported the results of an experiment in which 30 centimeter radiation was beamed at a discharge tube 3 cm in diameter and the back-scattered signal observed. Romell observed pronounced back scattering at several values of discharge tube current. He measured only relative values of the back-scattered signal, and was, therefore, unable to obtain any quantitative relation between the magnitude of the signal and the parameters describing the plasma.

It appeared that it would be of interest to perform an experiment in which the properties of the plasma resonance of an ionized column could be more carefully studied. Such an experiment was performed by placing a cylindrical section of a gaseous discharge tube between the conductors of a parallel plate transmission line. Theoretical relations were developed connecting the reflection coefficient measured on the line with the characteristics of the gaseous discharge. A description of the experiment and a comparison of the theoretical and experimental results is presented here.

## II THEORETICAL RELATIONS

### A. Nomenclature

A	Arbitrary constant
B	Arbitrary constant
$B_n$	Nth order scattering amplitude
B/A	Reflection coefficient
C	Capacitance per unit width
D	Scattering diameter
E	Electric field strength
H	Magnetic field strength
$H_n^{(1)}$	Hankel function, nth order, first kind
$H_n^{(1)'} $	Derivative of $H_n^{(1)}$ with respect to its argument
I	Current in discharge tube
$J_n$	Bessel function, nth order
$J_n' $	Derivative of $J_n$ with respect to its argument
K	Dielectric constant relative to free space
M	Line dipole moment
M'	Line dipole moment

$M''$	Line dipole moment
$N_e$	Number of electrons per unit length
$P_n^m$	Associated Legendre polynomial
$Q$	Charge per unit width
$R$	Function of radius only
$T_e$	Electron temperature
$U$	Potential function of complex potential
$V$	Stream function of complex potential
$W$	Complex potential, $W = U + iV$
$W_l$	Complex potential, line charge between planes
$Z_o$	Characteristic impedance
$Z_s$	Shunt impedance
$a$	Cylinder radius
$a'$	Fractional radius
$a_n$	Constant depending on $n$
$a_s$	Constant depending on $s$
$b$	Outer cylinder radius; Distance between planes
$d$	Width of parallel plate line



e	Charge on electron; Base of natural logarithms
g	Ellipse parameter, $g = (m^2 - n^2)^{1/2}$
i	Imaginary unit, $\sqrt{-1}$
j	Current density
k	Propagation constant
k'	Propagation constant in medium of $\epsilon'$
$k_n(q)$	Constant depending on $n$ and $q$
m	Mass of electron; Semi-major axis of ellipse; Index of summation
n	Electron concentration; Mode number; Index of summation; Semi-minor axis of ellipse
$n_0$	Electron concentration at cylinder axis
$\bar{n}$	Mean electron concentration
$n_u$	Electron concentration for resonance in uniform plasma
p	Arbitrary constant
$p_0$	Gas pressure reduced to $0^\circ\text{C}$
q	Index of summation
r	Radius in cylindrical coordinates $r, \phi, z$ , and spherical coordinates $r, \theta, \phi$
s	Index of summation
t	Time
u	Distance from plane to charge
v	Velocity

x	Coordinate position, rectangular coordinates x,y,z
y	Coordinate position, rectangular coordinates x,y,z
z	Coordinate position, rectangular coordinates x,y,z
$\alpha$	Angle; Parameter describing non-uniform plasma
$\beta$	Damping factor for Plasma, $\beta = \nu_c/\omega$
$\gamma$	Parameter describing non-uniform dielectric constant
$\delta$	Fractional length, dimensionless
$\epsilon$	Dielectric constant
$\epsilon'$	Dielectric constant of plasma
$\epsilon_0$	Dielectric constant of free space
$\epsilon_c$	Dielectric constant at cylinder axis
$\theta$	Colatitude angle in spherical coordinates r, $\theta$ , $\phi$
$\lambda$	Free space wavelength; Electron mean free path
$\mu_0$	Permeability of free space
$\nu_c$	Collision frequency
$\phi$	Scalar potential
$\varphi$	Polar angle in cylindrical coordinates r, $\varphi$ ,z; Azimuth angle in spherical coordinates r, $\theta$ , $\varphi$
$\omega$	Circular frequency

Note: All formulas are in rationalized MKS units.

## B. Dielectric Properties of a Plasma

The dielectric properties of an ionized plasma have been extensively studied theoretically (9-11) and experimentally (11-13). An idealized treatment of the problem is presented here primarily for reference.

In the plasma of an electrical discharge, positively and negatively charged particles are present in equal numbers. In the type of discharge considered the negative particles are electrons and the positive are ions. However, the mass of the lightest positive ion is almost 2000 times that of an electron, whereas they carry the same charge. As a consequence, the electric forces on electrons and ions are the same, but the motions induced by an electric field are thousands of times greater for electrons than for ions. For this reason it is permissible to treat the plasma as though it were composed of electrons only.

It is customary to neglect magnetic forces in comparison to electric forces. This is justified if the imposed frequency is high compared to the gyro-magnetic frequency (roughly 1 megacycle in the earth's field), and the induced velocity small compared to the velocity of light.

The equation of motion of an electron is given by

$$m \frac{dv}{dt} + m \nu_c v = e E$$

where  $m$  is the electron mass,  $e$  the charge on the electron, and  $v$  the velocity of the electron;  $E$  is the electric field, and  $\nu_c$  is the collision frequency. It may be seen that  $m \nu_c v$  is a retarding or damping force. Its form was suggested by Eccles (14) in 1912. Everhart and Brown (10) show that under certain conditions Marganeaus' results (9)

reduce to this form at sufficiently high frequency.

If all quantities vary as  $e^{-i\omega t}$ ; the electrons equation of motion may be written

$$-i\omega m v + m \nu_c v = E e$$

which may be solved to give

$$v = \frac{E e}{m(\nu_c - i\omega)} .$$

If  $n$  is the electron concentration, the current density  $j$  is given by  $nev$ , hence the current density may be written

$$j = \frac{ne^2 E}{m(\nu_c - i\omega)} .$$

If this result is substituted in Maxwell's Equation  $\nabla \times H = j - i\omega\epsilon_0 E$  there is obtained

$$\nabla \times H = \frac{ne^2 E}{m(\nu_c - i\omega)} - i\omega\epsilon_0 E$$

which may be written

$$\nabla \times H = -i\omega\epsilon_0 \left[ 1 - \frac{ne^2}{m\epsilon_0(\omega^2 + \nu_c^2)} + i \frac{\nu_c}{\omega} \frac{ne^2}{m\epsilon_0(\omega^2 + \nu_c^2)} \right] E .$$

If the presence of the electrons is considered to modify the dielectric constant, then Maxwell's Equation may be written  $\nabla \times H = -i\omega\epsilon' E$ , where

$$\epsilon' = \epsilon_0 \left[ 1 - \frac{ne^2}{m\epsilon_0(\omega^2 + \nu_c^2)} + i \frac{\nu_c}{\omega} \frac{ne^2}{m\epsilon_0(\omega^2 + \nu_c^2)} \right] . \quad (1)$$

It should be noted that the modified dielectric constant is complex, having an imaginary part if collisions are present. It should be noted

also that the effect of the presence of the plasma is to decrease the dielectric constant of free space. This is different from nearly all real dielectric substances, which have dielectric constants greater than that of free space. If the electron concentration is large enough or the frequency low enough, the dielectric constant may become negative. It should also be noted that a plasma is a strongly dispersive medium, since its properties are frequency dependent.

### C. The Equations Governing Scattering

In this section the equations describing the scattering of a plane wave by an infinite cylindrical plasma will be presented. The case where the electron concentration is a function only of the radial distance from the center of the cylinder will be considered.

Maxwell's Equations are, using the results of the last section

$$\nabla \times E = i\omega \mu_0 H \quad , \quad \nabla \times H = -i\omega \epsilon' E \quad .$$

Taking the curl of each gives

$$\nabla \times \nabla \times E = i\omega \mu_0 \nabla \times H \quad , \quad \nabla \times \nabla \times H = -i\omega \nabla \times \epsilon' E \quad .$$

The curl must operate on  $\epsilon'$ , since it is taken to be a function of position. Using the vector identity

$$\nabla \times \epsilon' E = \nabla \epsilon' \nabla \times E + \epsilon' \nabla \times E$$

and substituting to get equations in  $E$  and  $H$  only,

$$\nabla \times \nabla \times E = i\omega \mu_0 (-i\omega \epsilon' E)$$

$$\nabla \times \nabla \times H = -i\omega \left( \nabla \epsilon' \times \frac{\nabla \times H}{-i\omega \epsilon'} + \epsilon' i\omega \mu_0 H \right) \quad .$$

At this point two separate cases can be distinguished. In the case where the electric vector of the incoming wave traveling in the positive

x direction, is parallel to the axis of the column, taken to be the z axis, all scattered radiation will have an electric vector with only a z component and the equation in E will become a scalar rather than a vector equation. Similarly, where the electric vector is perpendicular to the axis of the cylinder, the H vector in the incoming and scattered radiation will have only a z component. In this case the equation in H will be a scalar equation. Writing for  $-\nabla^2$  for  $\nabla \times \nabla \times$  and  $k^2$  for  $\omega_{\mu_0}^2 \epsilon_0$ , there are obtained

$$(\nabla^2 + k^2) E = -k^2 \left( \frac{\epsilon'}{\epsilon_0} - 1 \right) E, \text{ parallel incidence}$$

$$(\nabla^2 + k^2) H = -k^2 \left( \frac{\epsilon'}{\epsilon_0} - 1 \right) H - \frac{\nabla \epsilon'}{\epsilon'} \times \nabla \times H, \text{ perpendicular incidence}.$$

Since  $\epsilon'$  is a function of only the radial distance  $r$ , these become, in cylindrical coordinates,  $r, \phi, z$

$$\frac{d^2 E}{dr^2} + \frac{1}{r} \frac{dE}{dr} + \frac{1}{r^2} \frac{d^2 E}{d\phi^2} + k^2 E = -k^2 \left( \frac{\epsilon'}{\epsilon_0} - 1 \right) E$$

and for the case of perpendicular incidence

$$\frac{d^2 H}{dr^2} + \frac{1}{r} \frac{dH}{dr} + \frac{1}{r^2} \frac{d^2 H}{d\phi^2} + k^2 H = -k^2 \left( \frac{\epsilon'}{\epsilon_0} - 1 \right) H + \frac{1}{\epsilon'} \frac{d\epsilon'}{dr} \frac{dH}{dr}. \quad (2)$$

It is the case of perpendicular incidence, where the electric vector of the plane wave is transverse to the axis of the cylinder, that may give rise to resonant scattering. No further reference will be made to the case of parallel incidence.

#### D. Scattering by a Homogeneous Dielectric Cylinder

If the electron concentration in a plasma is uniform, the dielectric constant within the plasma is not a function of position. It is possible in this case to consider a long cylindrical column of plasma to be an infinitely long homogeneous cylinder of dielectric material, its dielectric constant being given by Equation 1. For the case of a plane wave incident upon such a cylinder, whose axis is normal to the direction of propagation, it is possible to obtain an expression for the scattered radiation by the Fourier-Lamé method.

Consider a plane wave traveling in the positive  $x$  direction, with electric field in the  $y$  direction, striking a cylinder of radius  $a$  and dielectric constant  $\epsilon'$  centered on the  $z$  axis. The incident magnetic field is taken to be of unit strength, and to vary as  $e^{ikx}e^{-i\omega t}$ . The scattered magnetic field,  $H$ , lies entirely in the  $z$  direction. A result given in Smythe (15), page 503, may be used to obtain  $H$ . After changing notation this becomes

$$H = \sum_{n=0}^{\infty} B_n H_n^{(1)}(kr) \cos n\phi \quad (3)$$

where

$$B_n = (2 - \delta_0^n) i^n \frac{J_n(ka)J'_n(k'a) - (\epsilon'/\epsilon_0)^{1/2} J'_n(ka)J_n(k'a)}{(\epsilon'/\epsilon_0)^{1/2} J_n(k'a)H_n^{(1)}(ka) - J'_n(k'a)H_n^{(1)'}(ka)}.$$

In the expressions above  $r$  and  $\phi$  are polar coordinates in the  $x$ - $y$  plane.  $J_n$  is the Bessel function of the  $n^{\text{th}}$  order and first kind.  $J'_n$  is the derivative of  $J_n$  with respect to its argument.  $H_n^{(1)}$  is the Hankel function of the first kind and  $H_n^{(1)'} its derivative with respect to its argument. The quantity  $k$  is equal to  $\omega(\mu_0\epsilon_0)^{1/2}$  or  $2\pi/\lambda$ ,  $\lambda$  being the wavelength of the incident radiation in free space.$

The quantity  $k'$  is equal to  $\omega(\mu_0 \epsilon')^{1/2}$ . The symbol  $\delta_0^n$  represents the Kronecker delta, equal to zero if  $n \neq 0$ , and unity if  $n = 0$ .

Each  $B_n$  represents the strength of the  $n^{\text{th}}$  mode of scattered radiation,  $n = 1$  corresponding to the dipole mode. The various  $B_n$  may be used to compute the scattering diameter of the cylinder. The scattering diameter is defined as the diameter of a fictitious cylinder which abstracts from the incident wave all the power contained in the portion of the wave front it subtends and reradiates this power in such a way as to duplicate the scattered radiation.

The total scattered power may be found by integrating the power per unit area around a cylinder of unit height and a very large radius. If this power is set equal to the power incident upon an area of unit height and width  $D$ , the quantity  $D$  so determined is the scattering diameter. It is usually expressed nondimensionally as  $kD$ . Since the incident radiation that produced the scattered field given by Equation 2 was assumed to be of unit amplitude, the procedure outlined will give

$$D = \lim_{r \rightarrow \infty} \int_0^{2\pi} H(r, \phi) H^*(r, \phi) 2\pi r dr$$

where  $H^*$  denotes the conjugate of  $H$ . Recalling that

$$\lim_{r \rightarrow \infty} H_n^{(1)}(kr) = \left(\frac{2}{\pi kr}\right)^{1/2} e^{ikr} e^{-\frac{2n+1}{4}\pi i}$$

we can write

$$D = \frac{4}{\pi k} \int_0^{2\pi} \sum_{n=0}^{\infty} B_n e^{i\psi} \cos n\phi \overline{\sum_{n=0}^{\infty} B_n e^{i\psi} \cos n\phi}^* d\phi$$

where  $\psi = kr - \frac{2n+1}{4}\pi$ .

It may be seen that only terms of the form  $B_n e^{i\psi} \overline{B_n e^{i\psi}}^*$  will survive the integration, since  $\int_0^{2\pi} \cos m\phi \cos n\phi d\phi = 0$ ,  $m \neq n$ .



Now noting that  $B_n e^{i\psi} \overline{B_n e^{i\psi}}^* = B_n B_n^* = |B_n|^2$ , the expression for scattering diameter may be written

$$D = \frac{4}{\pi k} \int_0^{2\pi} \sum_{n=0}^{\infty} |B_n|^2 \cos^2 n\varphi d\varphi$$

or

$$kD = 4 \sum_{n=0}^{\infty} (1 + \delta_0^n) |B_n|^2 \quad . \quad (4)$$

From Equation 4, it is apparent that each  $B_n$  contributes to the scattering diameter according to the square of its modulus.

#### E. Scattering by a Thin Cylinder

It is of interest to determine the scattering properties of a cylinder whose radius is very much smaller than a wavelength. Using the series representations valid for small values of the argument to represent the various Bessel functions in Equation 3

$$\lim_{ka \rightarrow 0} B_n = \frac{-i^n}{1 + i \frac{(n!)^2 2^{2n}}{n\pi} \frac{1}{(ka)^{2n}} \frac{(\epsilon'/\epsilon_0) + 1}{(\epsilon'/\epsilon_0) - 1}}, \quad n > 0 \quad (5)$$

and  $\lim_{ka \rightarrow 0} B_0 = 0$  for any ratio  $\frac{\epsilon'}{\epsilon_0}$ .

It may be seen that if  $\frac{\epsilon'}{\epsilon_0} = -1$ ,  $B_n = 1$  independent of the value of  $n$ . This indicates that for very small values of  $ka$ , each mode is scattered equally when  $\frac{\epsilon'}{\epsilon_0} = -1$ , and the scattering diameter is infinite. This rather remarkable result appears more reasonable when the expression for  $\epsilon'$  given in Equation 1 is examined. It is seen that if  $\nu_c > 0$ , then  $\frac{\epsilon'}{\epsilon_0}$  cannot become equal to -1, but must always have an imaginary part. The ratio  $\nu_c/\omega$  may be considered a damping

factor for the plasma. Introducing the quantity  $\beta$ , where

$\beta = \nu_c / \omega$ , Equation 1 may be written

$$\epsilon' = \epsilon_0 \left[ 1 - \frac{ne^2}{m\epsilon_0(\omega^2 + \nu_c^2)} (1 - i\beta) \right].$$

If  $n$ , the electron concentration, is such that the real part of  $\epsilon'$  becomes  $-\epsilon_0$ , then

$$\frac{\frac{\epsilon'}{\epsilon_0} + 1}{\frac{\epsilon'}{\epsilon_0} - 1} \approx \frac{2i\beta}{-2 - 2i\beta} \approx -i\beta \quad \beta \ll 1$$

and

$$|\beta_n| \approx \frac{1}{1 + \frac{(n!)^2 2^{2n}}{n\pi} \frac{\beta}{(ka)^{2n}}}.$$

From this expression for  $|\beta_n|$  it may be seen that for any finite  $\beta$ , no matter how small, the amplitude of the higher order modes will vanish and the scattering diameter remain finite. To consider a numerical case take  $ka = .1$  and  $\beta = .01$ . These parameters represent a cylindrical plasma having a diameter about  $1/30$  of the wavelength of the incident radiation, with a collision frequency of about  $1/20$  the frequency of the incident radiation. For this case  $|B_1| \approx .9$  and  $|B_2| \approx .003$ . It is apparent that by far the greatest contribution to the scattering diameter is from the dipole mode. But even with only the dipole mode contributing the scattering diameter is much larger than the physical diameter. It may be seen from Equation 4 that in this case the scattering diameter  $D \approx \lambda/2$ , more than fifteen times the actual diameter of the cylinder.

## F. Quasi-Static-Resonances of Other Shapes

It has been shown that resonance exists for a column whose radius is vanishingly small compared to a wavelength. This indicates that some insight into the nature of the phenomena may be gained by consideration of situations in which radiation effects are neglected. This will give information concerning the field distributions and resonant frequencies, but can, of course, give no information on the damping due to radiation.

Starting with the problem of a cylinder of radius  $a$  and dielectric constant  $\epsilon'$  immersed in a medium of constant  $\epsilon_o$ , the potential outside the cylinder may be expressed as  $A r^{-n} \cos n\phi$  and the potential inside as  $B r^n \cos n\phi$ , where  $A$  and  $B$  are arbitrary constants. By equating potentials and normal displacements at the surface of the cylinder the equations

$$A a^n \cos n\phi = B a^{-n} \cos n\phi$$

$$\epsilon' n A a^{n-1} \cos n\phi = -n B \epsilon_o a^{-n-1} \cos n\phi$$

are obtained. These may be simplified to read

$$a^{2n} A - B = 0$$

$$\epsilon' a^{2n} A + \epsilon_o B = 0$$

which is satisfied if

$$\begin{vmatrix} a^{2n} & -1 \\ a^{2n} \epsilon' & \epsilon_o \end{vmatrix} = 0$$

$$\text{or } \epsilon' = -\epsilon_o.$$

Hence, all the possible modes of free oscillation are satisfied by the same value of  $\epsilon'$ , and all occur at the same frequency. This will serve to explain the scattering behavior of a cylinder as found previously.

For a dielectric sphere, the potential outside may be taken as  $Ar^{-(n+1)} P_n^m(\cos \theta) \sin m\phi$ , and that inside as  $Br^n P_n^m(\cos \theta) \sin m\phi$ . Here spherical coordinates are used, with  $\theta$  being the colatitude angle, and  $P_n^m$  the associated Legendre function. The same procedure used for the cylinder gives the result

$$\epsilon' = -\frac{n+1}{n} \epsilon_0.$$

For a sphere of plasma the various modes possible do not all occur at the same frequency. To produce dipole resonance, it is necessary that  $\epsilon' = -2\epsilon_0$ .

For an infinite half-space of dielectric  $\epsilon'$  occupying the region  $x > 0$ , the region  $x < 0$  being free space, with dielectric constant  $\epsilon_0$ , the following potentials may be used. For  $x > 0$ ,  $\phi = A e^{-px} \sin py$ ; for  $x < 0$ ,  $\phi = B e^{bx} \sin py$ . Here  $\phi$  is the potential, and  $A$ ,  $B$ , and  $p$  are arbitrary constants. Equating potentials and normal displacements at the boundary gives the result

$$\epsilon' = -\epsilon_0.$$

It is instructive to consider the case of an elliptic cylinder to further illustrate the dependence of plasma resonance on the shape of the plasma and its manner of excitation.

In Smythe (15), page 97, an expression is derived for the potential outside of an elliptic cylinder under the influence of a uniform field. Changing notation slightly the potential is given by

$$W = \frac{1}{2} E \left\{ \epsilon^{-i\alpha} \left[ z + (z^2 - g^2)^{1/2} \right] + (A'' \cos \alpha + iA' \sin \alpha) \left[ z - (z^2 - g^2)^{1/2} \right] \right\}.$$

In the expression above, the field of strength  $E$  makes an angle  $\alpha$  with the major axis of the cylinder.  $W$  is a complex potential  $U + iV$ ,  $U$  being the potential function and  $V$  the stream function. The coordinate position is  $z = x + iy$ , and the major axis of the ellipse lies along the  $x$  axis. The quantities  $A'$  and  $A''$  are given by

$$A' = \frac{-(m+n) \left( \frac{\epsilon'}{\epsilon_0} m - n \right)}{(m-n) \left( \frac{\epsilon'}{\epsilon_0} m + n \right)}$$

$$A'' = \frac{(m+n) \left( m - \frac{\epsilon'}{\epsilon_0} n \right)}{(m-n) \left( m + \frac{\epsilon'}{\epsilon_0} n \right)}$$

where  $\epsilon'$  is the dielectric constant of the cylinder,  $\epsilon_0$  the constant of free space,  $m$  the semi-major axis of the ellipse, and  $n$  its semi-minor axis. The quantity  $g$  is determined by  $g^2 = m^2 - n^2$ .

If in the equation for  $W$ , only very large values of  $z$  are considered, the approximation  $(z^2 - g^2)^{1/2} \approx z \left( 1 - \frac{g^2}{2z^2} \right)$  may be used. The corresponding expression for  $W$  becomes

$$W = E \left\{ \epsilon^{j\alpha} \left[ z + \frac{g^2}{4z} (A \cos \alpha + jA' \sin \alpha - 1) \right] \right\}.$$

If  $\alpha = 0$ , the field is aligned the major axis of the ellipse and

$$W = E \left\{ z + \frac{g^2}{4z} (A'' - 1) \right\}$$

when  $\alpha = \frac{\pi}{2}$ , the field is aligned with the minor axis of the ellipse and

$$W = E \left\{ z + \frac{g^2}{4z} (A' - 1) \right\}.$$

The potential of a line dipole of moment  $M$  per unit length is given by

$$W = \frac{M}{2\pi\epsilon_0} \frac{1}{z}.$$

Hence it may be seen that if the major axis is aligned with the field,

there is an equivalent induced dipole moment  $M'' = \frac{\pi \epsilon_0 g^2}{2} (A'' - 1)$  ,

whereas for the minor axis aligned with the field, the equivalent dipole

moment  $M' = \frac{\pi \epsilon_0 g^2}{2} (A' - 1)$  .

These dipole moments may be expressed as

$$M'' = \frac{\pi \epsilon_0 (m + n)}{2} E \left\{ \frac{(m+n)(m - \frac{\epsilon'}{\epsilon_0} n) - (m-n)(m + \frac{\epsilon'}{\epsilon_0} n)}{m + \frac{\epsilon'}{\epsilon_0} n} \right\}$$

$$M' = \frac{\pi \epsilon_0 (m + n)}{2} E \left\{ \frac{(m+n)(n - \frac{\epsilon'}{\epsilon_0} m) - (n-m)(m + \frac{\epsilon'}{\epsilon_0} n)}{\frac{\epsilon'}{\epsilon_0} m + n} \right\} .$$

If the field is along the major axis, the induced dipole becomes infinite and resonance occurs when  $\epsilon' = -\frac{m}{n} \epsilon_0$  . For the field along the minor axis, resonance occurs when  $\epsilon' = -\frac{n}{m} \epsilon_0$  . If  $m = n = a$  , the case reduces to that of a circular cylinder and the dipole moment becomes

$$M'' = M' = -2\pi \epsilon_0 a^2 E \frac{\frac{\epsilon'}{\epsilon_0} - 1}{\frac{\epsilon'}{\epsilon_0} + 1} \quad (6)$$

and resonance occurs when  $\epsilon' = -\epsilon_0$  , a result obtained previously.

From these results it is seen that the frequency of plasma resonance depends not only on the shape of the plasma but on the mode of oscillation excited by the external field.

## G. Gaseous Discharge Tube in a Parallel Plate Line

1. The Idealized Case. In an experiment in which an obstacle is placed in the vicinity of the conductors of a transmission line, some of the properties of the obstacle may be deduced from its position relative to

the line together with a measurement of the reflection coefficient produced by the obstacle.

In the case where a voltage wave of the form  $Ae^{ikx}$ , traveling in the positive  $x$  direction, encounters an obstacle at  $x = 0$ , a reflected wave of the form  $Be^{-ikx}$  will be generated. The quotient  $B/A$ , a complex quantity in general, is called the reflection coefficient or reflection factor. If the obstacle is considered to present to the line an equivalent shunt impedance  $Z_s$ , and the characteristic impedance of the line is  $Z_o$ , then the reflection coefficient is given by:

$$\frac{B}{A} = - \frac{1}{1 + 2 \frac{Z_s}{Z_o}} \quad (7)$$

In the quasi-static case the field in the neighborhood of the obstacle is found by solving Laplace's equation. The equivalent shunt impedance is given by  $i/\omega C$ , where  $C$  is the added capacitance that may be considered to exist at the location of the obstacle due to its presence.

To find the capacitance induced by a dielectric rod midway between the plates of a parallel plate transmission line, consider the width of the line to be very great compared to its spacing, and consider a typical section in a plane at right angles to the plates and parallel to the axis of propagation. The problem is thus reduced to the two-dimensional situation of parallel planes with a dielectric rod between them, its axis parallel to the planes.

The problem may be set up as follows. A dielectric rod of radius  $a$  and dielectric constant  $\epsilon'$  has its center at the origin in the complex  $z$  plane. Located at  $x = b/2$  and  $x = -b/2$  are conducting planes. In the region remote from the rod a potential of the form

$W = Ez$  exists in the region between the planes. To find the equivalent capacitance it is necessary to find the charge induced on the conducting planes by the rod.

In the case where the diameter of the rod is very much smaller than the distance between the planes, this may be approximated by finding the dipole moment induced in the rod by a uniform field in free space, and replacing the rod by this equivalent line dipole.

In Smythe (15), page 86, an expression is given for the potential due to a line charge between parallel conducting planes. Changing notation slightly this may be written

$$W_1 = - \frac{i}{\pi \epsilon_0} \tan^{-1} \left[ \tanh \frac{\pi z}{2b} \cot \frac{\pi u}{2b} \right] .$$

Here  $W_1$  is the complex potential, the conducting planes are at  $y = 0$ , and  $y = b$ . A line charge of unit strength per unit length is located at  $z = iu$ . The potential  $W$  due to a line dipole of strength  $M$  at  $y = u$  may be found as follows

$$W = M \frac{dW_1}{du} = \frac{iM}{2b\epsilon_0} \frac{\tanh \frac{\pi z}{2b} \csc^2 \frac{\pi u}{2b}}{1 + \tanh^2 \frac{\pi z}{2b} \cot^2 \frac{\pi u}{2b}} . \quad (8)$$

The charge  $Q$  induced by the dipole on the plane  $y = 0$  may be expressed as

$$Q = \epsilon_0 \left[ V(x = \infty, y = 0) - V(x = -\infty, y = 0) \right]$$

since  $V$  is the stream function. Noting that  $\lim_{x \rightarrow \pm\infty} \tanh \frac{\pi z}{2b} = \pm 1$ , the equation for  $Q$  becomes



$$Q = \epsilon_o \cdot \frac{M}{2b \epsilon_o} \left[ \frac{\csc^2 \frac{\pi u}{2b}}{1 + \cot^2 \frac{\pi u}{2b}} - \frac{-\csc^2 \frac{\pi u}{2b}}{1 + \cot^2 \frac{\pi u}{2b}} \right]$$

$$Q = \frac{M}{b} \quad . \quad (9)$$

It may be seen that the charge induced does not depend on  $u$ , the location of the dipole. As a consequence the charge induced by a multipole of high order is zero, since such a multipole may be constructed by a superposition of dipoles. In other words, the position of the dipole affects only the distribution of charge, but not its total amount, so the total charge induced by any multipole comprised of equal and opposite dipoles is zero. This result will be used later.

Using Equation 6, which gives the dipole moment induced in a cylinder by a uniform field, the expression for  $Q$  may be written

$$Q = \frac{2\pi \epsilon_o E a^2}{b} \frac{\frac{\epsilon'}{\epsilon_o} - 1}{\frac{\epsilon'}{\epsilon_o} + 1} \quad .$$

Since the capacitance  $C$  is equal to  $\frac{Q}{Eb}$  and  $Z_s = \frac{i}{\omega C}$ , the shunt impedance per unit width becomes

$$Z_s = \frac{i b^2}{2\pi \omega \epsilon_o a^2} \frac{\frac{\epsilon'}{\epsilon_o} + 1}{\frac{\epsilon'}{\epsilon_o} - 1} \quad .$$

For a parallel plate line, whose width  $d$  is great compared to its spacing  $b$ , a result in Smythe (15), page 466, gives for the characteristic impedance

$$Z_o = \sqrt{\frac{\mu_o}{\epsilon_o}} \frac{b}{d} \quad .$$

The reflection coefficient may be calculated from the expressions for  $Z_s$  and  $Z_o$ . Using Equation 7, and the relation  $k = \omega(\mu_o \epsilon_o)^{1/2}$

$$\frac{B}{A} = \frac{-1}{1 + \frac{i}{\pi} \frac{b}{a} \frac{1}{ka} \frac{\frac{\epsilon'_o}{\epsilon_o} + 1}{\frac{\epsilon'_o}{\epsilon_o} - 1}} \quad (10)$$

It should be noted that the expression for  $\frac{B}{A}$  is very similar to that for  $B_1$ , the amplitude of the dipole mode scattering of a small cylinder in free space, since from Equation 5

$$B_1 = \frac{-i}{1 + \frac{4i}{\pi} \frac{1}{(ka)^2} \frac{\frac{\epsilon'_o}{\epsilon_o} + 1}{\frac{\epsilon'_o}{\epsilon_o} - 1}}$$

The expressions cannot be derived from each other, since they apply to different physical situations.

2. Effect of Quasi-Static Approximation. It is difficult to account rigorously for the effect of using a quasi-static solution. In general, it is customary to take such a solution as satisfactory if all distances of importance are small compared with  $\lambda/2\pi$ .

In the case of a cylinder of radius  $a$  between the plates of parallel plate line, the excitation of the cylinder by the traveling wave is not in phase at all points on the cylinder. The phase difference in radians across the diameter of the cylinder is given by  $\frac{2a}{\lambda} \cdot 2\pi$ , which is  $2ka$ .

The charge induced on the plates by the cylinder is spread out rather than concentrated at the center line of the cylinder. The extent

of this spreading out may be estimated from Equation 8, giving the potential between the parallel planes due to a dipole between them. Placing the dipole midway between the planes, the potential becomes

$$W = \frac{iM}{2\epsilon_0 b} \frac{\tanh \frac{\pi z}{2b} \csc^2 \frac{\pi}{4}}{1 + \tanh^2 \frac{\pi z}{2b} \cot^2 \frac{\pi}{4}}$$

where  $W$  is the complex potential, the planes being at  $y = 0$  and  $y = b$ . This may be simplified to give

$$W = \frac{M}{2\epsilon_0 b} \tanh \frac{\pi z}{b}.$$

The charge  $Q'$  induced on the lower plane between  $x = a$  and  $x = -a$  is given by

$$Q' = \frac{M}{\epsilon_0 b} \tanh \frac{\pi a}{b}.$$

From Equation 9 the total charge induced on the plate is  $\frac{M}{\epsilon_0 b}$ . The fraction of the total charge included in a distance  $a$  either side of the center of the cylinder is then  $\tanh \frac{\pi a}{b}$ . For a cylindrical plasma whose diameter is half the distance between the plates of the transmission line, 90% of the induced charge is concentrated in a distance equal to the diameter of the plasma. For such a cylinder a significant dimension pertaining to the spreading out of charge may be taken to be  $2a$ . The ratio of this distance to the quantity  $2\pi/\lambda$  is  $2ka$ .

For the experiments to be described, the quantity  $2ka$  had a value of .14 at 300 megacycles, and it is assumed that this is sufficiently small compared to unity to permit the use of a quasi-static solution.

3. Effect of Non-Uniform Plasma Density. Equation 2, the differential equation governing scattering for the case of perpendicular incidence, is difficult to solve if the dielectric constant is not uniform. Interest in the problem has centered on the Gaussian distribution,  $n = n_0 e^{-(r/a)^2}$ , since this is assumed to represent the electron concentration in a meteor trail. Mackinson and Slade (16) attempted to approximate the solution by breaking the column up into five regions, adjusting the concentration in each to approximate a Gaussian distribution. They then employed the Fourier-Lame method to solve the problem. Their results indicated the presence of five resonant frequencies. The applicability of this result was questioned by Keitel (17) who cited a paper of his own (18). Keitel performed numerical computations on a high-speed digital computer to obtain scattering amplitudes for columns having Gaussian distributions of electron density. His results for a column of  $ka = .1$ ,  $\beta = 10^{-4}$  did not indicate any appreciable resonant response. The same quantity of electrons uniformly distributed over a column of radius  $a$  would display a very strong resonance.

Herlofson (2) attacked the problem by considering a uniform cylindrical plasma surrounded by a thin shell in which the electron concentration dropped linearly to zero. He concluded that the presence of concentration gradient would reduce the amplitude of the scattering coefficient and broaden the resonant peak. Herlofson's results are of uncertain use if the thickness of the shell is not small compared to the radius of the column, and do not represent any obtainable physical situation very closely.

In a gaseous discharge tube the electron concentration is usually taken (19) to be  $n_0 J_0 \left( \frac{2.4r}{a+a'} \right)$  where  $r$  is the radius within the

cylindrical plasma,  $a$  the radius of the confining tube, and  $a'$  a length related to the mean free path.  $J_0$  is the Bessel function of zero order. This distribution is very close to that given by  $n_0(1 - \alpha \frac{r^2}{a^2})$  where  $\alpha = 1 - J_0(\frac{2.4a}{a+a'})$ . A solution for this parabolic distribution of electron density may be obtained using the quasi-static approximation.

Equation 2, being a differential equation in  $H$ , the magnetic field, is of no utility in the quasi-static approximation. The differential equation to be satisfied may be derived from Maxwell's equation  $\nabla \cdot D = \nabla \cdot \epsilon' E = 0$ . Using the vector identity  $E \cdot \nabla \epsilon' + \epsilon' \nabla \cdot E = 0$ , and defining the potential  $\phi$  by  $E = -\nabla \phi$ , there is obtained  $\nabla^2 \phi + \frac{1}{\epsilon'} \nabla \phi \cdot \nabla \epsilon' = 0$ . In cylindrical coordinates, with  $\epsilon'$  a function of  $r$  only, this equation becomes

$$\frac{d^2 \phi}{dr^2} + \left( \frac{1}{r} + \frac{1}{\epsilon'} \frac{d\epsilon'}{dr} \right) \frac{d\phi}{dr} + \frac{1}{r^2} \frac{d^2 \phi}{d\phi^2} = 0.$$

If a product solution of the form  $\phi = R(r) \cos \phi$  is assumed, this differential equation may be written

$$\frac{d^2 R}{dr^2} + \left( \frac{1}{r} + \frac{1}{\epsilon'} \frac{d\epsilon'}{dr} \right) \frac{dR}{dr} - \frac{R}{r^2} = 0.$$

If  $\epsilon' = \epsilon_c(1 - \gamma r^2)$ , the differential equation becomes

$$\frac{d^2 R}{dr^2} + \left( \frac{1}{r} - \frac{2\gamma r}{1 - \gamma r^2} \right) \frac{dR}{dr} - \frac{1}{r^2} R = 0.$$

Recognizing that when  $\gamma = 0$ , this equation is solved by  $\phi = Ar$ , a solution of the form  $R = Ar g(r)$  is substituted. This gives a differential equation for  $g(r)$

$$(1 - \gamma r^2) g''(r) + \left(\frac{3}{r} - 5\gamma r\right) g'(r) - 2\gamma g(r) = 0 .$$

If a series solution of the form  $g(r) = \sum_{s=0}^{\infty} a_s r^s$  is substituted, it is found that

$$g(r) = a_0 + \gamma a_2 r^2 + \gamma^2 a_4 r^4 + \dots + \gamma^s a_{2s} r^{2s} + \dots$$

$$\text{where } a_{s+2} = \frac{s^2 + 4s + 2}{(s+2)(s+4)} a_s .$$

If at  $r = 1$  the dielectric constant changes abruptly to that of free space, then a criterion for resonance may be determined. Assuming a potential outside the cylinder of the form  $\frac{B}{r} \cos \theta$  and equating potentials and normal displacements at the boundary, the criterion for resonance becomes

$$\epsilon_c = -\epsilon_0 \frac{g(1)}{(1 - \gamma) [g(1) + g'(1)]} = -\epsilon_0 f(\gamma) .$$

This quantity may be related to  $\alpha$ , the parameter in the equation for electron concentration by recalling Equation 1 relating dielectric constant to electron concentration. If the electron concentration necessary to produce resonance in a uniform cylinder is denoted by  $n_u$ , and collisions are neglected, equation 1 becomes

$$\epsilon' = \epsilon_0 \left[ 1 - \frac{2n}{n_u} \right] = \epsilon_0 \left[ 1 - \frac{2n_0(1 - \alpha \frac{r^2}{a^2})}{n_u} \right] .$$

Since it has been assumed that  $\epsilon' = \epsilon_c(1 - \gamma \frac{r^2}{a^2})$ , the relations between the various parameters become

$$\epsilon_c = \epsilon_0 \left[ 1 - \frac{2n_0}{n_u} \right] , \quad \gamma = \frac{-2 \frac{n_0}{n_u} \alpha}{1 - \frac{2n_0}{n_u}} .$$

Using the criterion for resonance  $\epsilon_c = -\epsilon_o f(\gamma)$  two relations may be obtained

$$\frac{n_o}{n_u} = \frac{1 + f(\gamma)}{2}, \quad \alpha = \frac{\gamma f(\gamma)}{1 + f(\gamma)}.$$

In a cylinder in which the electron concentration is given by

$$n_o \left(1 - \alpha \frac{r^2}{a^2}\right), \text{ the mean electron concentration } \bar{n} \text{ is given by } \bar{n} = n_o \left(1 - \frac{\alpha}{2}\right).$$

From this the equation

$$\frac{\bar{n}}{n_u} = \left(1 - \frac{\alpha}{2}\right) \frac{1 + f(\gamma)}{2}$$

may be written.

Figure 1 shows graphically the relation between  $\frac{\bar{n}}{n_u}$  and  $\alpha$ . It may be seen that for small departures from uniform concentration the mean electron density necessary for resonance is almost unchanged. For  $\alpha = .11$ , corresponding to the experimental situation at a mercury vapor pressure of  $1.54 \times 10^{-3}$  mm (see section on "Properties of a Gaseous Discharge"), the necessary increase in electron density is only .12%. Therefore no correction is made for non-uniform plasma density.

4. Effect of Finite Cylinder Radius. To calculate the capacitance that is added by the dielectric rod when its radius is comparable to the spacing, it is necessary to take account of the fact that the field due to the presence of the rod produces a redistribution of charge on the planes.

In order to accomplish this an iterative procedure may be utilized.

First, the field from the rod induced by the uniform field between the planes may be found. Next, the effect on this field due to the presence of the planes may be obtained. The effect of the rod on the

additional field of the planes may then be found. This process may then be repeated as often as necessary. The procedure is similar to that used by Smythe (15) page 118, for finding the field in the neighborhood of two spheres by successive iteration of images. A step-by-step illustration of the procedure is given in Figure 2.

A complex potential  $W$  outside of the rod but due to its presence may be expressed as

$$W = \sum_{n=1}^{\infty} \frac{C_n}{z^n}$$

since the rod contains no net charge and its field must die off at infinity. Each  $C_n$  may be related to the strength of an  $n$ th order multipole located at the origin. Of all these multipoles, only the dipole, corresponding to  $n = 1$ , can induce net charge on the planes.

If a field due to the charges on the planes is expressed as

$$W = \sum_{n=1}^{\infty} A_n z^n$$

which is permissible since the field must be finite at the origin, then a relation may be written between the components  $A_n$  of an external field due to charges on the planes, and the components  $C_n$  of the field produced from it by the dielectric rod. This relation may be obtained by equating potentials and the normal displacements at the surface of the rod, and is given by

$$C_n = - A_n a^{2n} \frac{\frac{\epsilon'}{\epsilon_0} - 1}{\frac{\epsilon'}{\epsilon_0} + 1}.$$

It may be seen that only the  $A_1$  term in the expression for the potential due to charges on the planes contributes to the induction of dipole moment



in the cylinder, the  $A_1$  term being the uniform field component of the potential between the planes.

The effect of the presence of the planes on the potential due to a multipole at the origin may be calculated by replacing them with an infinite set of images of the multipole located at  $x = \pm mb$ ,  $m$  ranging from one to infinity. If the potential of a multipole at the origin is given by  $C_n z^{-n}$ , the potential due to the presence of the planes may be expressed as

$$W = C_n \sum_{m=1}^{\infty} \frac{1}{(z + mb)^n} + \frac{1}{(z - mb)^n}.$$

It is desirable to express this in the form of  $W = \sum_{r=1}^{\infty} A_r z^r$ , since this will be necessary for the iterative procedure to be followed. By the use of Maclaurin's Series

$$W = \sum_{r=1}^{\infty} A_r z^r = \sum_{r=1}^{\infty} \frac{W^{(r)}(0)}{r!} z^r$$

where  $W^{(r)}(0)$  represents the  $r$ th derivative of  $W(z)$ , evaluated at  $z = 0$ . Proceeding formally

$$W = C_n \sum_{m=1}^{\infty} \frac{1}{(z + mb)^n} + \frac{1}{(z - mb)^n}$$

$$\frac{dW}{dz} = C_n \sum_{m=1}^{\infty} \frac{-n}{(z + mb)^{n+1}} + \frac{-n}{(z - mb)^{n+1}}$$

$$\frac{d^2W}{dz^2} = C_n \sum_{n=1}^{\infty} \frac{n(n+1)}{(z + mb)^{n+2}} + \frac{n(n+1)}{(z - mb)^{n+2}}$$

$$\frac{d^r W}{dz^r} = C_n (n+r-1)(n+r-2) \cdots (n) \sum_{m=1}^{\infty} \frac{(-1)^r}{(z+mb)^{n+r}} + \frac{(-1)^r}{(z-mb)^{n+r}}$$

$$W_r(0) = C_n (n+r-1)(n+r-2) \cdots (n) \sum_{m=1}^{\infty} \frac{(-1)^r}{(mb)^{n+r}} + \frac{(-1)^r}{(-mb)^{n+r}}$$

$$W^r(0) = \frac{(-1)^r C_n (n+r-1)(n+r-2) \cdots n}{b^{n+r}} \sum_{m=1}^{\infty} \frac{1 + (-1)^{n+r}}{m^{n+r}}$$

hence for  $n+r$  odd,  $W^r(0) = 0$ , and for  $n+r$  even

$$W^r(0) = \frac{(-1)^r 2 C_n (n+r-1)(n+r-2) \cdots (n)}{b^{n+r}} \sum_{m=1}^{\infty} \frac{1}{m^{n+r}}$$

but by a well-known relationship, (20)

$$\sum_{m=1}^{\infty} \frac{1}{m^{n+r}} = \frac{\pi^{n+r} 2^{n+r-1}}{(n+r)!} B_{\frac{n+r}{2}} \quad n+r \text{ even}$$

where  $B_n$  is the Bernoulli Number,  $B_1 = 1/6$ ,  $B_2 = 1/30$ , etc. and

hence

$$W^r(0) = \frac{(-1)^r \pi^{n+r} 2^{n+r} B_{\frac{n+r}{2}}}{b^{n+r} (n+r) (n-1)!} C_n \quad n+r \text{ even}$$

and finally  $W = \sum_{r=1}^{\infty} A_r z^r$ , where  $A_r = \frac{W^r(0)}{r!}$ , so

$$A_r = \frac{(-1)^r \pi^{n+r} 2^{n+r} B_{\frac{n+r}{2}}}{b^{n+r} (n+r) (n-1)! r!} C_n \quad n+r \text{ even}$$

This together with the previously obtained relation  $C_n = -a^{2n} \frac{\frac{\epsilon'}{\epsilon} - 1}{\frac{\epsilon'}{\epsilon} + 1} A_n$ ,  
 $\epsilon_0$

is all that is needed to proceed with the iteration procedure.

First, the uniform field between the plates has a potential given by  $W = E z$ , hence for this field only  $A_1$  exists and its value is given by  $E$ . This is the first term in the expression for the total uniform field.

The corresponding field due to the presence of the rod is given by

$$W = \frac{C_1}{z}, \quad C_1 = -a^2 \frac{\frac{\epsilon'_0}{\epsilon_0} - 1}{\frac{\epsilon'_0}{\epsilon_0} + 1} E$$

all other  $C_n$  being zero.

The field produced by the presence of the plates may be expressed as

$$W = \sum_{r=1}^{\infty} A_r z^r, \quad A_r = a^2 \frac{\frac{\epsilon'_0}{\epsilon_0} - 1}{\frac{\epsilon'_0}{\epsilon_0} + 1} E \sum_{r=1,3,5}^{\infty} \frac{\pi^{r+1} 2^{r+1} B_{\frac{r+1}{2}}}{b^{r+1} (r+1)!}$$

since only  $C_1$  exists.

The important  $r = 1$  term giving the second contribution to the uniform field is

$$W = E \frac{\pi^2}{3} \frac{a^2}{b^2} \frac{\frac{\epsilon'_0}{\epsilon_0} - 1}{\frac{\epsilon'_0}{\epsilon_0} + 1}.$$

The multipoles that are produced from this field by the rod are given by

$$W = \sum_n C_n z^{-n} = -a^2 \left( \frac{\frac{\epsilon'_0}{\epsilon_0} - 1}{\frac{\epsilon'_0}{\epsilon_0} + 1} \right)^2 E \sum_{n=1,3,5}^{\infty} \frac{a^{2n} \pi^{n+1} 2^{n+1} B_{\frac{n+1}{2}}}{b^{n+1} (n+1)!} z^{-n}.$$

This in turn induces charges on the plates. The desired  $A_1$  term is given by

$$A_1 = a^2 \left( \frac{\frac{\epsilon'}{\epsilon_0} - 1}{\frac{\epsilon'}{\epsilon_0} + 1} \right)^2 E \sum_{n=1,3,5} \frac{a^{2n} \pi^{2n+2} \left( \frac{B_{n+1}}{2} \right)^2}{b^{2n+2} (n+1)! (n+1) (n-1)!}.$$

This is equivalent to

$$A_1 = \left( \frac{\pi^2}{3} \right)^2 \left( \frac{a^2}{b^2} \right)^2 \left( \frac{\frac{\epsilon'}{\epsilon_0} - 1}{\frac{\epsilon'}{\epsilon_0} + 1} \right)^2 E \left[ 1 + \frac{\pi^4}{2 \cdot 3^4 \cdot 5^2} \frac{a^4}{b^4} + \frac{\pi^8}{3^6 \cdot 5^2 \cdot 7^2} \frac{a^8}{b^8} + \dots \right]$$

It may be seen that qth repeated application of the iteration process will give a similar result which can be expressed as

$$A_1(q) = \left( \frac{\pi^2}{3} \right)^q \left( \frac{a^2}{b^2} \right)^q \left( \frac{\frac{\epsilon'}{\epsilon_0} - 1}{\frac{\epsilon'}{\epsilon_0} + 1} \right)^q \left[ 1 + k_4(q) \frac{a^4}{b^4} + k_8(q) \frac{a^8}{b^8} + \dots \right]$$

where  $k_4, k_8, \dots$ , will be functions of  $q$  only. As the process is continued they will each approach a limiting value as the fields become more similar. The total uniform field may be written as

$$A_1 = E \sum_{q=0}^{\infty} \left( \frac{\pi^2}{3} \right)^q \left( \frac{a^2}{b^2} \right)^q \left( \frac{\frac{\epsilon'}{\epsilon_0} - 1}{\frac{\epsilon'}{\epsilon_0} + 1} \right)^q \left[ 1 + k_4(q) \frac{a^4}{b^4} + k_8(q) \frac{a^8}{b^8} + \dots \right]$$

where  $q$  becomes large  $k_4(q), k_8(q), \dots$ , will approach limiting values,  $k_4, k_8, \dots$ .

To evaluate the value of the sum  $1 + k_4 \frac{a^4}{b^4} + k_8 \frac{a^8}{b^8} + \dots$ , the case of a conducting cylinder may be considered. In this case  $\frac{\epsilon'}{\epsilon_0}$  becomes infinite and the factor  $(\epsilon'/\epsilon_0) - 1 / (\epsilon'/\epsilon_0) + 1$  becomes unity. In the case of the limiting value  $\frac{a}{b} = \frac{1}{2}$ , when the conducting cylinder is just touching the planes, the field must become infinite. Hence we can write

$$\frac{\pi^2}{3} \left(\frac{1}{2}\right)^2 \cdot 1 \left[ 1 + k_4 \left(\frac{1}{2}\right)^4 + k_8 \left(\frac{1}{2}\right)^8 + \dots \right] = 1$$

or

$$\left[ 1 + k_4 \left(\frac{1}{2}\right)^4 + k_8 \left(\frac{1}{2}\right)^8 + \dots \right] = \frac{12}{\pi^2} = 1.2158 \quad .$$

In order to evaluate the contribution of this series for smaller values of  $\frac{a}{b}$ , note that the excess over the value unity must decrease at least as rapidly as  $\left(\frac{a}{b}\right)^4$ . Hence for a rod whose diameter is half the distance between the planes, the maximum value the series can have is  $1 + \frac{.2158}{16}$  or 1.0135. As a consequence, the total field for values of  $\frac{a}{b}$  less than  $\frac{1}{4}$  is given to an accuracy of better than 1.5% by the expression

$$A_1 = E \sum_{q=0}^{\infty} \left(\frac{\pi^2}{3}\right)^q \left(\frac{a^2}{b^2}\right)^q \left(\frac{\frac{\epsilon'}{\epsilon_0} - 1}{\frac{\epsilon'}{\epsilon_0} + 1}\right)^q \quad .$$

This expression can be written as

$$A_1 = \frac{E}{1 - \frac{\pi^2}{3} \frac{a^2}{b^2} \frac{\frac{\epsilon'}{\epsilon_0} - 1}{\frac{\epsilon'}{\epsilon_0} + 1}} \quad .$$

From Equation 6, the total dipole moment  $M$  induced is given by

$$M = \frac{2\pi \epsilon_0 a^2 E \frac{\frac{\epsilon'}{\epsilon_0} - 1}{\frac{\epsilon'}{\epsilon_0} + 1}}{1 - \frac{\pi^2}{3} \frac{a^2}{b^2} \frac{\frac{\epsilon'}{\epsilon_0} - 1}{\frac{\epsilon'}{\epsilon_0} + 1}} \quad .$$

Since by Equation 9, the total charge  $Q$  induced on plates a distance  $b$  apart by a dipole of strength  $M$  is  $\frac{M}{b}$  and since  $C = \frac{Q}{E b}$ , the

capacitance per unit width due to the presence of the dielectric rod is given by

$$C = 2\pi \epsilon_0 \frac{a^2}{b^2} \frac{\frac{\epsilon'}{\epsilon_0} - 1}{\frac{\epsilon'}{\epsilon_0} + 1} \frac{1}{1 - \frac{\pi^2}{3} \frac{a^2}{b^2} \frac{\frac{\epsilon'}{\epsilon_0} - 1}{\frac{\epsilon'}{\epsilon_0} + 1}} .$$

Hence Equation 10, giving the reflection coefficient in the idealized case, must be modified to include the effect of finite cylinder radius. The reflection coefficient becomes

$$\frac{B}{A} = \frac{-1}{1 + \frac{i}{\pi} \frac{b}{a} \frac{1}{ka} \frac{\frac{\epsilon'}{\epsilon_0} + 1}{\frac{\epsilon'}{\epsilon_0} - 1} \left( 1 - \frac{\pi^2}{3} \frac{a^2}{b^2} \frac{\frac{\epsilon'}{\epsilon_0} - 1}{\frac{\epsilon'}{\epsilon_0} + 1} \right)} . \quad (11)$$

5. Effect of Finite Tubing Thickness. In the laboratory, an approximately uniform plasma must be produced in a confined cylinder. The characteristics of the tube that confines the discharge have an effect on the phenomena observed.

Following the method used by Smythe (15) in finding the scattering due to a uniform dielectric cylinder, the scattered radiation from a cylinder of radius  $a$  and dielectric constant  $\epsilon'$ , surrounded by a concentric cylindrical shell of outer radius  $b$  and dielectric constant  $\epsilon''$  may be found. The result is as given in Equation 3 except that  $B_n$  is modified. For this case the expression for  $B_n$  becomes

$$B_n = -i^n (2 - \delta_0^n) \frac{J_n(kb) [A - B] - J_n'(kb) [C - D]}{H_n^{(1)}(kb) [A - B] - H_n^{(1)'}(kb) [C - D]}$$

where

$$\begin{aligned}
 A &= \frac{1}{\epsilon''} J_n(k'a) \left\{ J_n'(k''b) Y_n(k''a) - Y_n'(k''b) J_n(k''a) \right\} \\
 B &= \left( \frac{1}{\epsilon' \epsilon''} \right)^{1/2} J_n'(k'a) \left\{ J_n'(k''b) Y_n(k''a) - Y_n'(k''b) J_n(k''a) \right\} \\
 C &= \left( \frac{1}{\epsilon_o \epsilon'} \right)^{1/2} J_n(k'a) \left\{ J_n(k''b) Y_n'(k''a) - Y_n(k''b) J_n'(k''a) \right\} \\
 D &= \left( \frac{1}{\epsilon_o \epsilon'} \right)^{1/2} J_n'(k'a) \left\{ J_n(k''b) Y_n(k''a) - Y_n(k''b) J_n(k''a) \right\} .
 \end{aligned}$$

If, in the expression above, the leading terms in the expansions for the Bessel Functions are substituted for the functions themselves, and  $n$  set equal to unity, the dipole mode scattering amplitude for small  $ka$  can be found. If the imaginary part of the denominator is set equal to zero, to make the modulus of the scattered dipole mode amplitude a maximum, the following equation is obtained:

$$\frac{b}{a} \left[ \frac{\epsilon'}{\epsilon''} + 1 + \frac{\epsilon'}{\epsilon_o} \right] = \frac{a}{b} \left[ \frac{\epsilon'}{\epsilon''} - 1 - \frac{\epsilon'}{\epsilon_o} + \frac{\epsilon''}{\epsilon_o} \right]$$

and if  $b = a(1 + \delta)$ ,  $\epsilon'' = K \epsilon_o$ , and terms in  $\delta^2$  are neglected

$$\epsilon' = -\epsilon_o \left[ 1 + \delta \left( K - \frac{1}{K} \right) \right] .$$

This same result may be obtained very simply by considering the quasi-static case of concentric dielectric cylinders. The radius of the inner cylinder is  $a$  and its dielectric constant  $\epsilon'$ , the radius of the outer cylinder  $b$  and its dielectric constant  $\epsilon''$ .

Potentials may be assumed of the form  $\frac{A}{r} \cos \theta$  outside the outer cylinder,  $\frac{B}{r} \cos \theta + Cr \cos \theta$  within the outer cylinder, and  $Dr \cos \theta$  within the inner cylinder. If potentials and normal displacements are equated at the boundaries, four equations are obtained. The determinant formed by the coefficients of the four unknowns may be set equal to

zero to give the relation for free oscillation.

Performing these operations results in the equation

$$\epsilon' = -\epsilon_0 \frac{\left(\frac{b^2}{a^2} + 1\right) + \frac{\epsilon''}{\epsilon_0} \left(\frac{b^2}{a^2} - 1\right)}{\left(\frac{b^2}{a^2} + 1\right) + \frac{\epsilon_0}{\epsilon''} \left(\frac{b^2}{a^2} - 1\right)} \quad (12)$$

If  $\frac{\epsilon''}{\epsilon_0}$  is set equal to  $K$ ,  $b$  equal to  $a(1 + \delta)$ , and terms in  $\delta^2$  are neglected, this expression becomes

$$\epsilon' = -\epsilon_0 \left[ 1 + \delta \left( K - \frac{1}{K} \right) \right]$$

which is identical to that previously obtained.

The effect of the dielectric walls is to require the inner dielectric constant to be more negative (the electron concentration greater) for resonance to occur than would be the case in their absence.

For the experiment described here, the tubing was No. 774 pyrex, having a relative dielectric constant of 4.3 at 300 megacycles. The ratio  $\frac{b}{a}$  was 1.143. Substituting these quantities in Equation 12 gives the result  $\epsilon' = -1.52 \epsilon_0$  at resonance.

6. Effect of Finite Line Width. In the idealized case it was assumed that the width of the parallel plate transmission line was very great compared to its spacing, and its characteristics were computed for a typical section. In a practical case these results may be modified by the presence of the edges of the plates.

Where the cylindrical plasma extends far beyond the edges of the plates, the degree of coupling of an element of length of the plasma to the plates falls off rapidly beyond the edges. This may be seen by



following a line of force from the top of the upper plate to the bottom of the lower plate. The potential difference along the line of force between the points where it enters and leaves the cylinder may be taken as a crude measure of the degree of coupling. The potential difference across a diameter of the cylinder decreases with increasing distance from the edge.

From the results in the discussion "Effect of Finite Cylinder Radius", it may be seen that the resonant frequency of the cylindrical plasma is modified by the presence of the parallel plates. For a dielectric cylinder of radius  $a$  in line of infinite width and spacing  $b$ , the dielectric constant for resonance is given by

$$\epsilon' = -\epsilon_0 \frac{1 + \frac{\pi^2 a^2}{3b^2}}{1 - \frac{\pi^2 a^2}{3b^2}},$$

whereas for the same cylinder in free space the dielectric constant for resonance would be  $\epsilon' = -\epsilon_0$ . It is apparent that each element of length of the plasma will contribute to the total shunt admittance, but that the magnitude and phase angle of its contribution will depend on the location of the element. The contribution of all the plasma outside the region between the plates may be approximately compared to that of the plasma within the region between the plates by a comparison of the relative contributions of these regions to the total capacitance per unit length of the transmission line.

If the plates of width  $d$  were very wide compared to their spacing  $b$ , the capacitance between them would be  $\epsilon_0 \frac{d}{b}$  per unit length. The

actual capacitance per unit length,  $C$  , may be found from a relation in Smythe (15), page 109.

$$C = \epsilon_0 \frac{K(k')}{K(k)} , \text{ where } \frac{K(k')E\left\{\cos^{-1} \frac{E(k')}{K(k')}, k'\right\} - E(k')F\left\{\cos^{-1} \frac{E(k')}{K(k')}, k'\right\}}{K(k)E(k') - \left(\frac{k}{k'}\right)^2 E(k)K(k')} = \frac{d}{b} .$$

Here  $E$ ,  $F$ , and  $K$  are the elliptic integrals whose moduli are  $k$  or  $k'$  , as indicated, and  $k^2 + k'^2 = 1$  . The transmission line used for the experiments described here had a ratio of  $b/d = 5.72$  . The approximation for  $C$  used in the idealized case gives a capacitance of  $5.72\epsilon_0$  per unit length, whereas the use of the exact expression results in a capacitance per unit length of  $7.22\epsilon_0$  . (This correlates well with the fact that the ratio  $b/d$  was adjusted to match 50 ohm line, which would theoretically require a capacitance of  $7.55\epsilon_0$  per unit length.) It may be seen from these figures that about 75% of the total capacitance may be attributed to the region between the plates.

Since the plasma outside the plates is less effective in producing shunt admittance than that between the plates, somewhat less than 25% of the total admittance will be due to the portion of the plasma not between the plates. It is difficult to make any quantitative modification of the results from the idealized case to account for this situation.

#### H. Properties of a Gaseous Discharge.

To predict the reflection coefficient due to the presence of a plasma in a transmission line it is necessary to know the mean electron concentration in the discharge tube, the radial variation of this concentration, and the collision frequency.

At present the state of understanding of the processes occurring in the cylindrical positive column or plasma of a gaseous discharge is such that only reasonably close numerical values may be calculated for these quantities. Experimental work in this field involves techniques of considerable difficulty. The disparity between the values obtained by different investigators for a quantity such as mean electron density may be as great as a factor of two. In general, however, the experimental values determined by careful investigators will fall within 30-40% of the value expected.

A rather complete theoretical treatment of the low pressure mercury vapor discharge, together with a summary of experimental results, is given by Klarfeld (21). Using his results, two important parameters of the discharge may be determined. The first of these is  $N_e/I$ , which is the number of electrons per unit length of the tube per ampere of discharge current. The second of these is  $T_e$ , the electron temperature. These are both functions of the quantity  $ap_0$ ,  $a$  being the radius of the discharge tube, and  $p_0$  the gas pressure reduced to  $0^\circ\text{C}$ .

The situation regarding the radial variation of electron density is somewhat less clear cut. Ambipolar diffusion theory indicates that the electron density should be given by  $n = n_0 J_0\left(\frac{2.4r}{a+a'}\right)$  where  $n_0$  is the density on the axis and  $a$  the radius of the tube. It can be shown (19) that if diffusion takes place for electrons of all energies, and if the mean free path is the same for electrons of all energies, then  $a' = 3/4 \lambda$ , where  $\lambda$  is the electron mean free path. While neither of these conditions is closely approximated in a typical mercury vapor discharge, Howe (19) measured radial distributions that agreed fairly well with the assumption that the mean free path was that computed by using

the collision cross section for electrons in mercury vapor measured by Brode (22) at an energy corresponding to the electron temperature. Radial distributions measured by Killian (23) do not fit this assumption as well. Nonetheless, it appears that this assumption offers a satisfactory method of calculating the radial variation of electron concentration in terms of the known parameters describing the discharge.

With regard to the collision frequency, the situation is also not clear cut. Margenau's (9) theory of the high frequency behavior of a plasma gives the complex conductivity for the assumption that the mean free path of electrons does not depend on their velocity. Everhart and Brown (11) show that for high frequencies Margenau's expression is equivalent to Equation 1. Adler (13) measured the complex conductivity of a mercury vapor discharge and concluded that the assumption of a mean free path independent of velocity gives satisfactory agreement with the measured complex conductivity. Adler computed a value for the mean free path of electrons in a mercury vapor discharge.

A reasonable procedure for predicting  $\beta$ , the damping factor for the plasma, is to use Margenau's theory together with Adler's measured value of the mean free path. This procedure gives the result

$$\beta = \frac{4}{3} \frac{\bar{c}}{\omega \lambda}$$

where  $\bar{c}$  is the mean velocity corresponding to the electron temperature  $T_e$ ,  $\bar{c} = \left(\frac{8kT_e}{\pi m}\right)^{1/2}$ ,  $k$  being Boltzmann's constant, and  $\lambda$  the mean free path of the electrons.

## J. Summary of Theoretical Relations

By use of Klarfeld's (21) relation connecting  $N_e/I$  with  $ap_0$ , the number of electrons per unit length of cylindrical plasma may be determined. The only quantities necessary for this determination are the discharge tube radius; the temperature of the condensed mercury; the temperature of the mercury vapor; and the discharge tube current. By use of equation 1 which relates the plasma dielectric constant,  $\epsilon'$ , to  $n$ , the electron concentration; the electron concentration necessary to produce the condition  $\epsilon' = -\epsilon_0$  may be determined. For this to be done the only experimental quantity that needs to be known is the frequency. If it is assumed that the plasma density in the discharge tube is uniform, and that resonance occurs when  $\epsilon' = -\epsilon_0$ , the discharge tube current that will produce resonance may be computed. This discharge current must be corrected to account for the various approximations made in obtaining the result  $\epsilon' = -\epsilon_0$  at resonance.

By use of Klarfeld's relation connecting  $T_e$ , the electron temperature, with  $ap_0$ ; together with the relation from kinetic theory  $\bar{c} = \left(\frac{8kT_e}{\pi m}\right)^{1/2}$  that relates electron temperature to mean electron velocity, the mean velocity may be determined. Using Brode's (22) data, a collision cross section corresponding to this velocity may be found. Using this cross section and the pressure  $p_0$ , a value of mean free path may be calculated. The quantity  $a'$ , which is necessary to compute electron concentration gradient, may be calculated from this mean free path. From  $a$  and  $a'$  the ratio of electron concentration at the wall to that at the axis may be calculated. For the experiment reported here, the smallest value of this ratio that was obtained from this procedure is .64, corresponding to a pressure of  $3.13 \times 15^3$  mm Hg.

From the section "Effect of Non-uniform Plasma Density" it may be seen that this corresponds to an increase of 2.5% in the electron concentration necessary for resonance. Since at all other pressures the correction is even smaller, no correction was made for non-uniform concentration.

It is shown in the section "Effect of Finite Tubing Thickness" that the presence of the pyrex tube used would cause resonance to occur  $\epsilon'/\epsilon_0 = -1.52$  .

It is shown in the section "Effect of Finite Cylinder Radius", that in a very wide line resonance would occur at  $\epsilon'/\epsilon_0 = -1.52$  , the ratio  $a/b = 1/4$  having been used in this experiment. It is shown in the section "Effect of Finite Line Width" that the correction for the finite width would reduce the excess over -1 by less than 25%. Since the amount of this reduction is uncertain, the full amount may be used.

The corrections due to tubing thickness and finite width both being small, it may be assumed that they are superimposable. This results in a figure  $\epsilon'/\epsilon_0 = -2.31$  at resonance.

The current required to produce an electron density corresponding to  $\epsilon'/\epsilon_0 = -2.31$  may be calculated by the method outlined previously. This procedure was used to give the theoretical curve in Figure 9, showing current for resonance versus frequency, and Figure 11, showing current for resonance versus gas pressure.

To calculate  $\beta$  , the damping factor of the plasma, a result of Adler (13) is utilized. From measurements of the complex conductivity in a mercury vapor discharge, he found that the assumption of a mean free path of  $9.5 \times 10^{-3}$  cm at 1 millimeter pressure gave agreement with his experimental results. (The pressure range covered by Adler's experiments overlapped but was generally higher than that used here.)

Using this mean free path, and the mean velocity corresponding to  $T_e$ , the factor  $\beta$  may be calculated from Margenau's results (9) given in the section "Properties of a Gaseous Discharge". This procedure was used to give the theoretical curve in Figure 10, showing  $\beta$  versus frequency, and Figure 12, showing  $\beta$  versus gas pressure.

From Equation 11, a value of  $\beta$  may be computed using the measured value of  $\left| \frac{B}{A} \right|$  at resonance. The calculated curves in Figure 7 showing  $\left| \frac{B}{A} \right|$  versus current, and Figure 8, showing the angle of  $\frac{B}{A}$  versus current, are simply plots of these quantities from Equation 11. These calculated curves were made without reference to values that might be obtained from the theory of the gas discharge.

### III EXPERIMENTAL APPARATUS AND TECHNIQUES

#### A. Choice of Experimental Method

Scattering experiments in free space require rather formidable techniques in order to obtain accurate results. One particular difficulty lies in separating the desired scattered radiation from energy scattered by miscellaneous objects in the vicinity of experimental area. A second difficulty is measuring the scattered radiation in the presence of the incident radiation.

A generally accepted technique involves the use of an artificial ground plane many wavelengths in extent. A probe is used to sample the total field in the neighborhood of the scattering specimen. All experimental apparatus other than the radiating antenna, the scattering object, and the probe are located below the ground plane. In general, the scatterer is bisected by the ground plane so only a half model is necessary.

While this technique is satisfactory for experiments involving three-dimensional scatterers, it leaves a great deal to be desired if

applied to the two-dimensional problem of scattering by an ionized column where the electric vector is transverse to the column. Also, apart from the two-dimensional nature of the problem, there are difficulties in applying the method to an ionized column formed by a gaseous discharge.

The basic trouble is that in the neighborhood of the ground plane the electric field is normal to the ground plane. This requires the axis of the column be parallel with the ground plane. If the ground plane is slotted to admit the column the fields in the neighborhood of the column are severely distorted. The ground plane cannot, of course, continue through the column as this would short out the voltage maintaining the discharge. If a discharge of special section is constructed, such that placed upon the ground plane it represents half a cylinder, then the ion concentration is no longer approximately uniform, in fact it does not even have radial symmetry. If the column is located some distance above the ground plane, then many of the advantages of the method are lost, since the necessary leads to the column and the probe disturb the fields.

In addition to the specialized difficulties caused by the scatterer being a gaseous discharge, there are those connected with the two-dimensional nature of the problem. It would be desirable to have the column at least several wavelengths long in order to reduce the importance of end effects. In addition the long column should be in an approximately plane wave, which means the radiator must be several column-lengths from the column. As a consequence of these two requirements the ground plane must be many wavelengths in extent to represent a satisfactory experimental situation.



The cost and complexity of applying the ground plane method to investigating the scattering of a plane wave incident on an ionized column with the electric vector transverse to the axis of the column, leads to examination of other experiments which may display the phenomena involved in free space reflection. The most obvious of these is to span a waveguide with a discharge in such a way that the axis of the discharge is transverse to the field.

Using a gaseous discharge tube in a waveguide has many features that make the experimental situation better than in free space. Since the energy is confined to the interior of the guide there are, in general, no radio frequency fields around the measuring apparatus. A wealth of conventional apparatus exists for measurement of standing wave ratio in waveguides. However, the dimensions of waveguide must be comparable to the wavelength of the radiation to be scattered or the guide will not propagate energy. This limits the use of this technique to relatively high frequencies, and, in turn, entails certain disadvantages. It is desirable to have the radius of the discharge tube small compared to a wavelength. The reason for this is the simplified theoretical interpretation of the experimental results that may be made. To make the quantity  $ka$  equal to 0.1 or less at 3000 megacycles, the radius of the discharge tube must be less than .16 cm. However, even for this small a diameter, no adequate theory is available for the effect of a dielectric rod in a waveguide with its axis transverse to the electric field.

Consideration of these difficulties led to examination of the possibility of conducting a scattering experiment in a parallel plate transmission line. A parallel plate line will allow propagation of a TEM wave of any frequency. Furthermore, if the line width is large compared to

the spacing, a nearly uniform electric field exists between the plates. Hence the field to which the discharge is exposed is almost identical to that seen by a column exposed to a plane wave in free space. With care the leakage of energy may be held to a low enough value so that no difficulty need be experienced from stray fields. It was felt that an experiment using a parallel plate line represented a good working compromise between the experimental difficulties of the free space methods and the restrictions implicit in the waveguide method.

#### B. Description of Apparatus

A parallel plate transmission line was designed and fabricated for this experiment. The line consisted of a uniform central section 48 inches long and tapered matching sections 20 inches long at each end. The matching sections were attached to the parallel plates by short strips of flexible shim stock to allow the taper to be adjustable. The pieces comprising each matching section were trapezoids, 10 inches wide where they were joined to the 10-inch wide uniform line, and  $3/4$  inches wide at the other end. The pieces comprising the line were fabricated of  $1/8$ -inch thick aluminum sheet. They were supported by insulators of adjustable length within a rigid wooden frame. By adjustment of the insulator heights the line spacing could be made uniform over its entire length, and the taper of the matching sections adjusted as required.

In the experiments reported here the central section of the line was set at 1.75 inches, with a maximum variation of .030 inch from point to point. The small ends of the matching sections were fastened directly to RG58A/U coaxial cable having 50 ohms characteristic resistance. Figure 3 is a photograph illustrating certain features of the construction of the transmission line assembly.

It was necessary to build a standing wave ratio indicator for the line. After several attempts, an indicator was designed that was sensitive enough to give satisfactory readings and yet was free from "hand capacity" effects. The sensing portion of the indicator was made of two small pieces of brass sheet, each of about  $1/3$  square inch area, placed about  $3/4$  inch apart. This sensing portion could be moved along the line in such a way that its plates moved parallel to the line while they projected into the space between the conductors of the line. The depth of projection into the line was constant within about .020 inch. A silicon diode, type 1N21B, was connected between the plates of the sensing probe, and each plate connected through a 500-ohm resistor to the conductors of a short coaxial cable.

At the other end of the cable the d.c. voltage that was developed across an 800-ohm resistor was read by an elementary potentiometer arrangement. The potential from a mercury cell, reduced to a suitable value, was applied to the terminals of a precision voltage divider, and the divider ratio set to null a sensitive galvanometer connected between the divider and the 800-ohm terminating resistor. By these means a divider reading proportional to the square of the voltage on the line could be made easily and accurately. Figure 4 is a photograph of the standing wave ratio indicator assembly.

A mercury vapor discharge tube was designed and fabricated for the purpose of providing the cylindrical plasma. The entire tube was 36 inches long, so when the tube was placed between the 10-inch wide plates of the line, both the anode and cathode were well removed from the high field region. An oxide-coated, electrically heated thermionic cathode was used. The entire cathode assembly was taken from a type 866A mercury vapor rectifier.

Two side arms were provided near the anode end of the tube. One was used as a mercury reservoir, and the second to provide a connection to the vacuum pumping system. A photograph of the discharge tube, Figure 5, shows the details of its construction.

In operation, the vacuum pump was run continuously. The pressure of mercury vapor in the discharge tube was very nearly the vapor pressure of mercury at the temperature of the constant temperature bath. This condition was assured by making the pumping speed of the line connecting the upper sidearm to the vacuum system very low compared to the pumping speed of the lower sidearm.

A General Radio Type 857-A oscillator was used as a source of radio frequency energy. It was isolated from the transmission line by a 10-decibel pad. The power transmitted through the line was absorbed in a 50-ohm terminating resistor.

Power for heating the filament and maintaining the discharge was supplied from well regulated supplies. A resistance of at least 1000 ohms was always used in series with the discharge tube.

A general view of the experimental apparatus, with each important component labeled, is shown in Figure 6.

### C. Calibration and Operating Technique

Before any data could be taken, it was necessary to minimize the residual standing wave ratio of the transmission line. This was easily accomplished by adjustment of the tapered matching sections. Sending and receiving ends were interchanged several times during this procedure to ensure the proper termination of both ends of the line. A residual standing wave ratio of 1.04 at 300 megacycles, and less than 1.15 at all

frequencies between 175 and 450 megacycles, was achieved.

The linearity of the standing wave indicator was checked by making a standing wave survey with the receiving end termination removed. For a perfect square law detector, the readings obtained would describe a wave of the form  $A(1 + \sin \frac{4\pi x}{\lambda})$ . The readings obtained showed a maximum deviation from this curve of less than  $\pm 1\%$  maximum reading.

A copper tube was placed in the line at the position to be occupied by the discharge tube. This was equivalent to the condition  $\epsilon' = \infty$  in Equation 11. The measured standing wave ratio was 1.17, versus a calculated value of 1.15.

During these preliminary standing wave surveys it was observed that the reading of the standing wave indicator was affected by only about two or three parts in 1000 due to movement of its cable, touching the galvanometer housing, moving about the room, etc. However, an attempt was made to minimize movement of any large conducting object in the vicinity of the line during the course of taking data.

The usual procedure in taking data was to fix the frequency of the oscillator, fix the temperature of the constant temperature bath, and, at a selected value of discharge current to record the maximum and minimum values read at the standing wave ratio indicator. From their ratio the magnitude of the reflection coefficient could be obtained. The mean of these values was then computed and the position of the probe on the line adjusted so as to produce a reading equal to this mean. This position was used to determine the phase angle of the reflection coefficient. The discharge current was then changed and the procedure repeated.

No time lag in reaching a steady state was observed following a

change in discharge current. When the temperature of the condensed mercury was changed, about one minute was required before equilibrium was attained.

The only inconvenience noted in operating the apparatus was the necessity for constant attention to the temperature bath. A temperature change of only  $.2^{\circ}\text{F}$  was sufficient to produce an observable change in standing wave ratio.

#### IV RESULTS AND DISCUSSION

Figures 7 and 8 show the results of a series of runs in which the discharge current was varied while the gas pressure and frequency were kept constant. The different symbols represent runs made on different days. Figure 7 shows voltage standing wave ratio as a function of discharge current. Voltage standing wave ratio is related to the modulus of the reflection coefficient,  $\left| \frac{B}{A} \right|$ , by the relation  $VSWR = \frac{1 + \left| B/A \right|}{1 - \left| B/A \right|}$ , and is a somewhat more familiar quantity than  $\left| \frac{B}{A} \right|$ . Figure 8 shows the argument or angle of the complex quantity  $\frac{B}{A}$  as a function of discharge current.

The calculated curves presented in Figures 7 and 8 are derived from Equation 11 only. Using this equation, the damping factor for the plasma,  $\beta$ , may be computed from the observed maximum value of  $\frac{B}{A}$ . If this quantity is substituted back in Equation 11, and use made of the fact that electron concentration is directly proportional to current, the modulus and argument of  $\frac{B}{A}$  at all values of discharge current may be calculated from the value of discharge current where  $\left| \frac{B}{A} \right|$  reaches its maximum.

It may be observed that the shapes of the experimental curves are significantly different from those calculated. Probably most of this difference is due to the effect of finite line width. In contrast to the experimental results of Tonks (6) and Romell (8), pronounced resonant response was observed at only one value of discharge current.

Figures 9 and 10 show the results of a series of runs in which the frequency was varied and the discharge current necessary to produce resonance observed. Figure 9 shows the theoretical current required for resonance compared with the experimental values observed. The difference

between the two values is somewhat greater than might be expected, but may be due to the approximations made by Klarfeld (21) in deriving the theory from which the theoretical curve was computed.

The damping factor  $\beta$ , shown in Figure 10 as a function of frequency, was computed from the standing wave ratio at resonance. The wide disagreement between the theoretical and experimental values is probably due to the effect of finite line width. The finite width causes the portion of the plasma remote from the plates to become resonant at a slightly lower current than that portion of the plasma between the plates. As a consequence the resonance is broadened and the apparent value of the damping factor,  $\beta$ , is increased.

Figures 11 and 12 show the results of a series of runs in which the gas pressure was varied and the discharge current necessary to produce resonance was observed. The disparity noted between the theoretical and experimental values is nearly in constant ratio at gas pressures in excess of about  $10^{-3}$  mm Hg. Below this pressure the curves are totally different. It would be of interest to make probe measurements of the electron density in the low gas pressure region in an effort to find a cause for this discrepancy.

Figure 12, showing  $\beta$  as a function of gas pressure, was computed from the standing wave ratio at resonance. As in the case of  $\beta$  versus frequency shown in Figure 10, the disagreement between the theoretical and experimental curves may be attributed to the effect of finite width.



V FIGURES

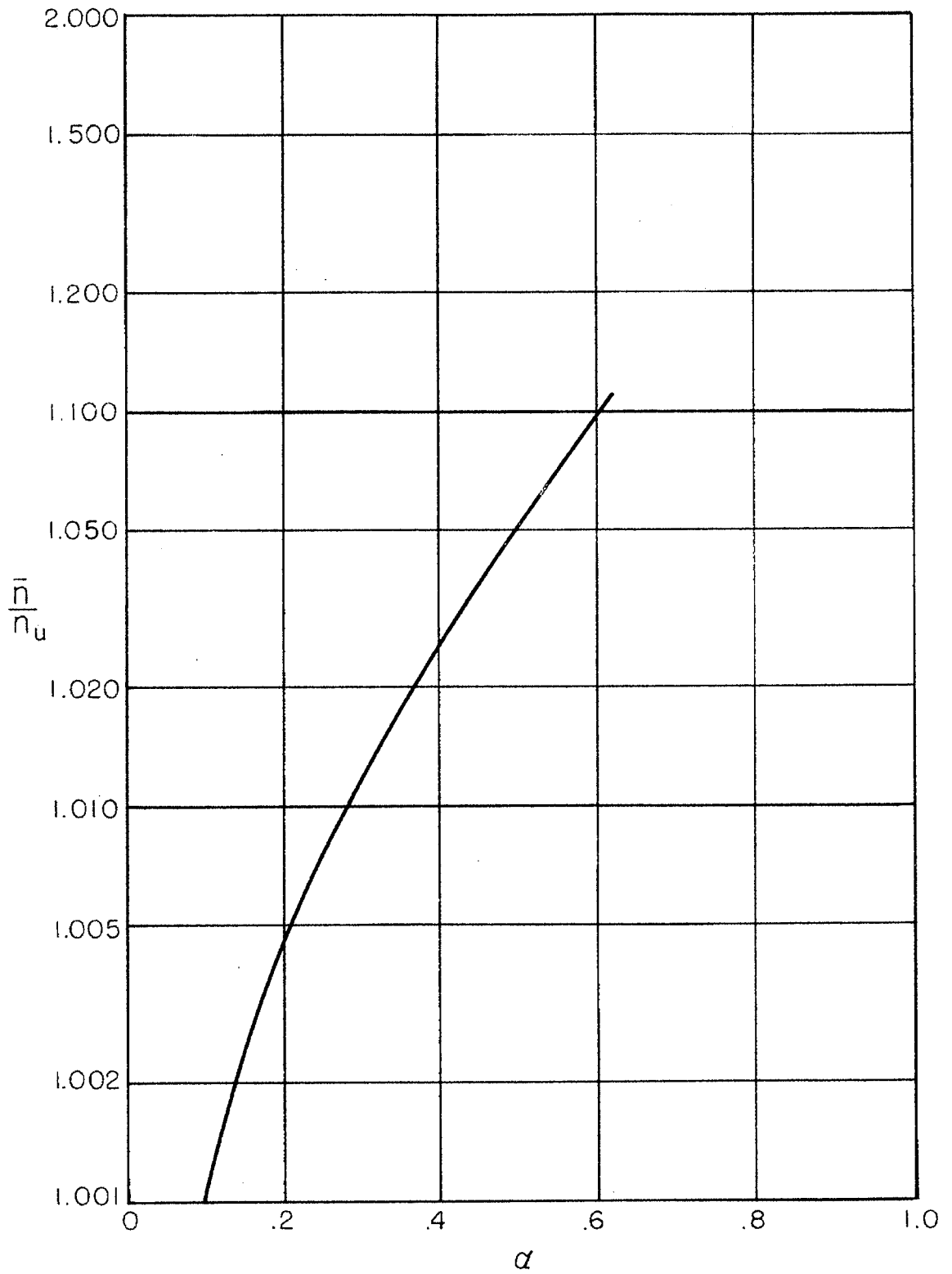


Figure 1. Mean Density for Resonance versus  $\alpha$

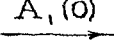


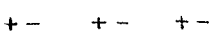
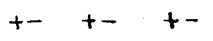
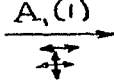



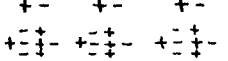
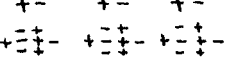
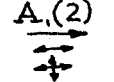

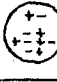

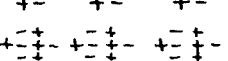
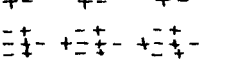



$A_1(0)$ 		Original uniform field extends throughout all space ...
		Satisfying the boundary condition on conducting plates, but not on conducting cylinder
		Introducing dipole satisfies b.c. on cylinder, but destroys b.c. on plates
		Introducing image dipoles restores b.c. on plates
$A_1(1)$ 		Images can be represented by the equivalent field at the origin expressed as a power series...
		which destroys the b.c. on the cylinder
		Introduce dipoles and multipoles to restore b.c. on cylinder
		But these again destroy the b.c. on the plates
		Restore b.c. on plates by an array of dipole and multipole images ...
$A_1(2)$ 		which can be represented by the equivalent field at the origin expressed as a power series ...
		which destroys the b.c. on the cylinder
		Introduce dipoles and multipoles to restore b.c. on cylinder
		But these again destroy the b.c. on the plates
		Restore b.c. plates by an array of dipole and multipole images...
$A_1(3)$ 		which can be represented by the equivalent field at the origin expressed as a power series...
		which destroys the b.c. on the cylinder
		Introduce dipoles and multipoles to restore b.c. on cylinder...

Figure 2. Illustration of Successive Images.

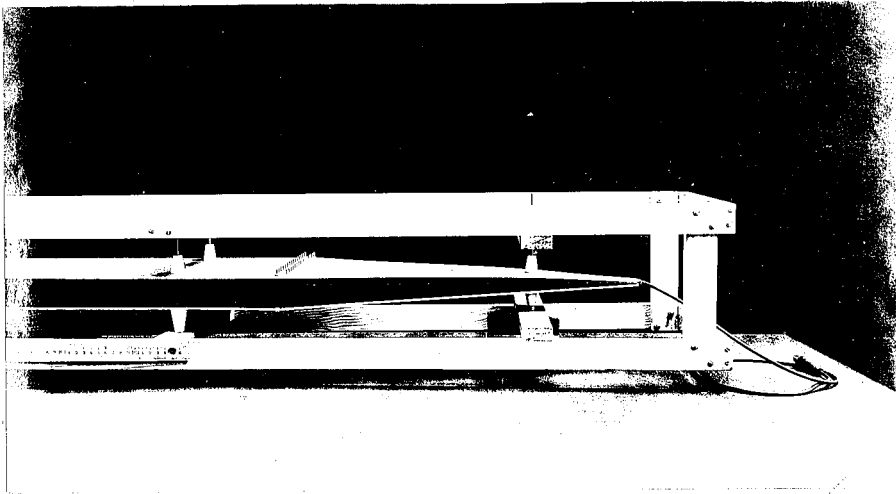


Figure 3. Details of Transmission Line

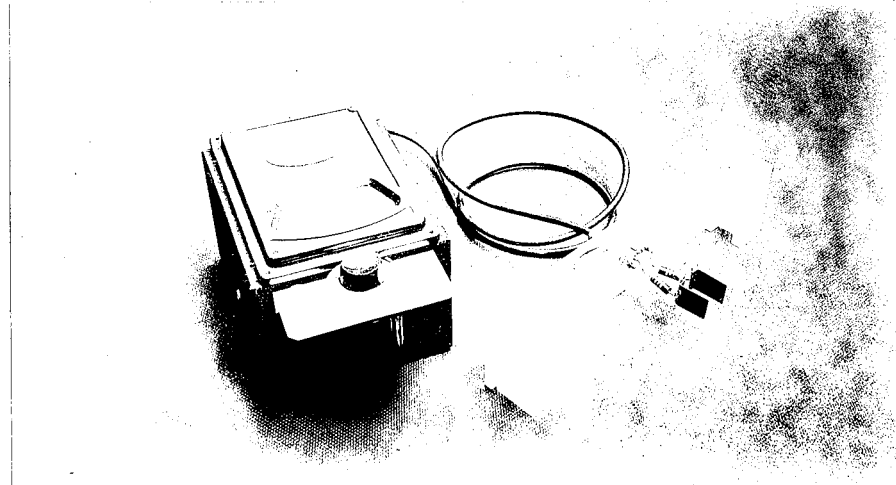


Figure 4. Standing Wave Ratio Indicator

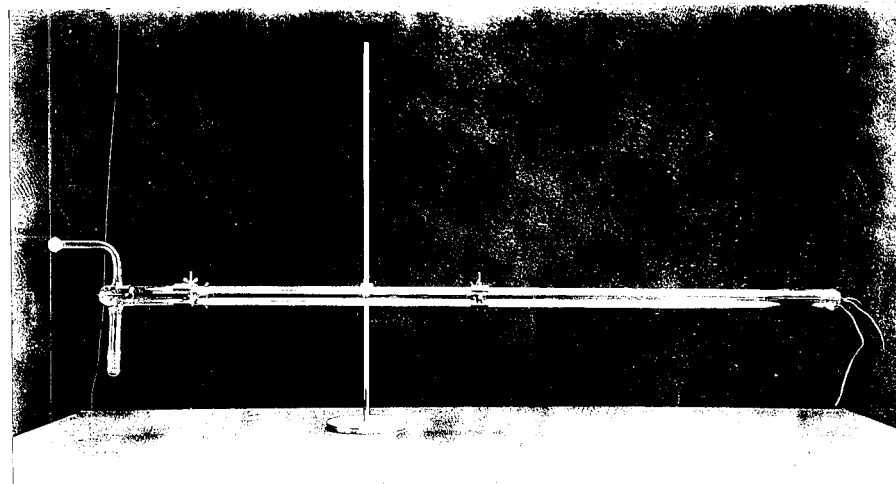


Figure 5. Gaseous Discharge Tube

# RESONANT PLASMA RESEARCH APPARATUS

- |  |  |
|--|--|
| 1 • DISCHARGE TUBE<br>A. HEATED CATHODE<br>B. ANODE                                  | 7 • TEMPERATURE BATH<br>8 • THERMOMETER<br>9 • METER STICK |
| 2 • TRANSMISSION LINE  | 10 • AMMETER   |
| 3 • OSCILLATOR   | 11 • VACUUM GAGE   |
| 4 • MERCURY POOL   | 12 • DIFFUSION PUMP  |
| 5 • TERMINATING RESISTOR   |  |
| 6 • STANDING WAVE RATIO INDICATOR<br>A. PROBE<br>B. POTENTIOMETER<br>C. GALVANOMETER |  |

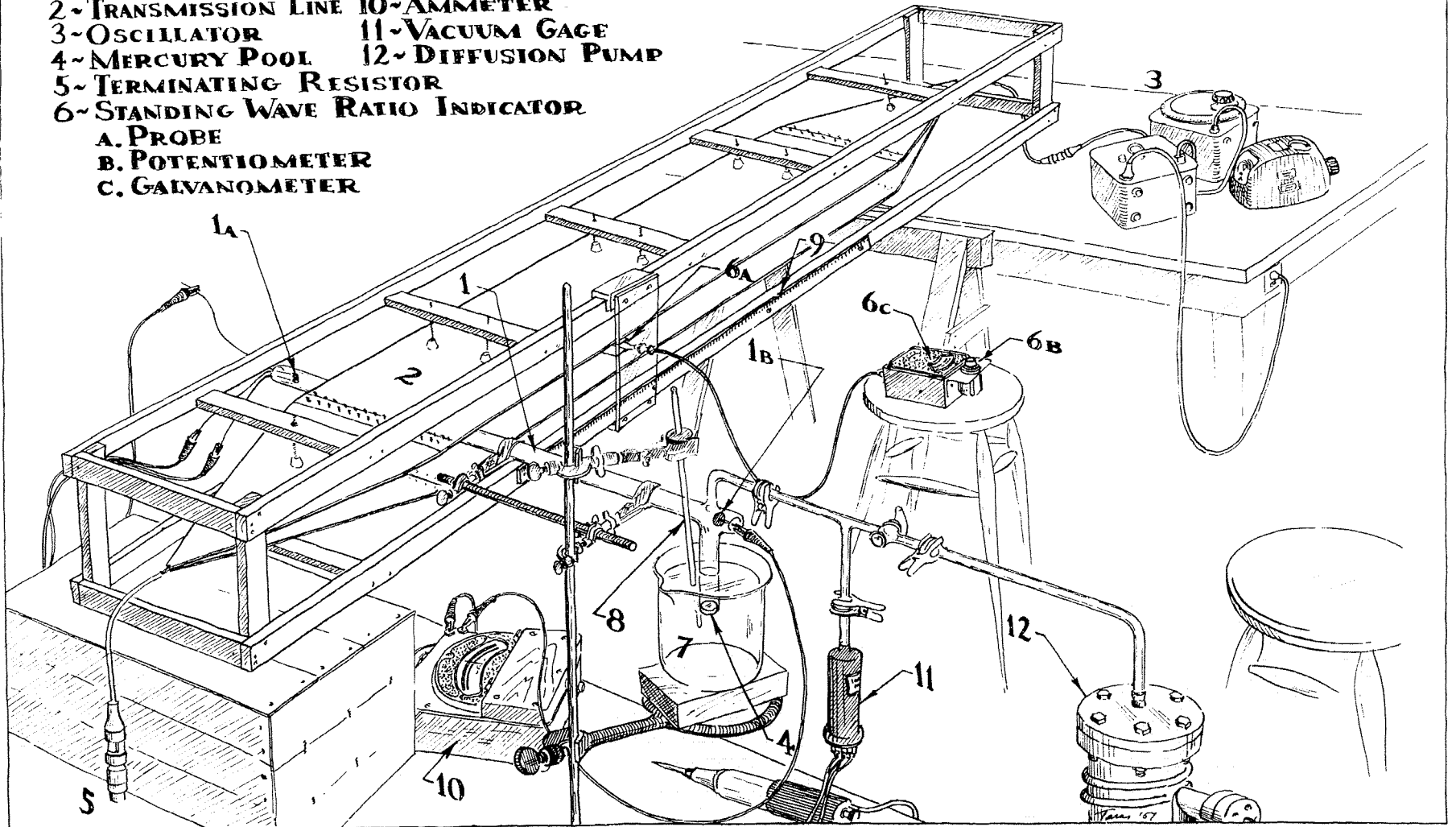


Fig.6 General View of Experimental Apparatus

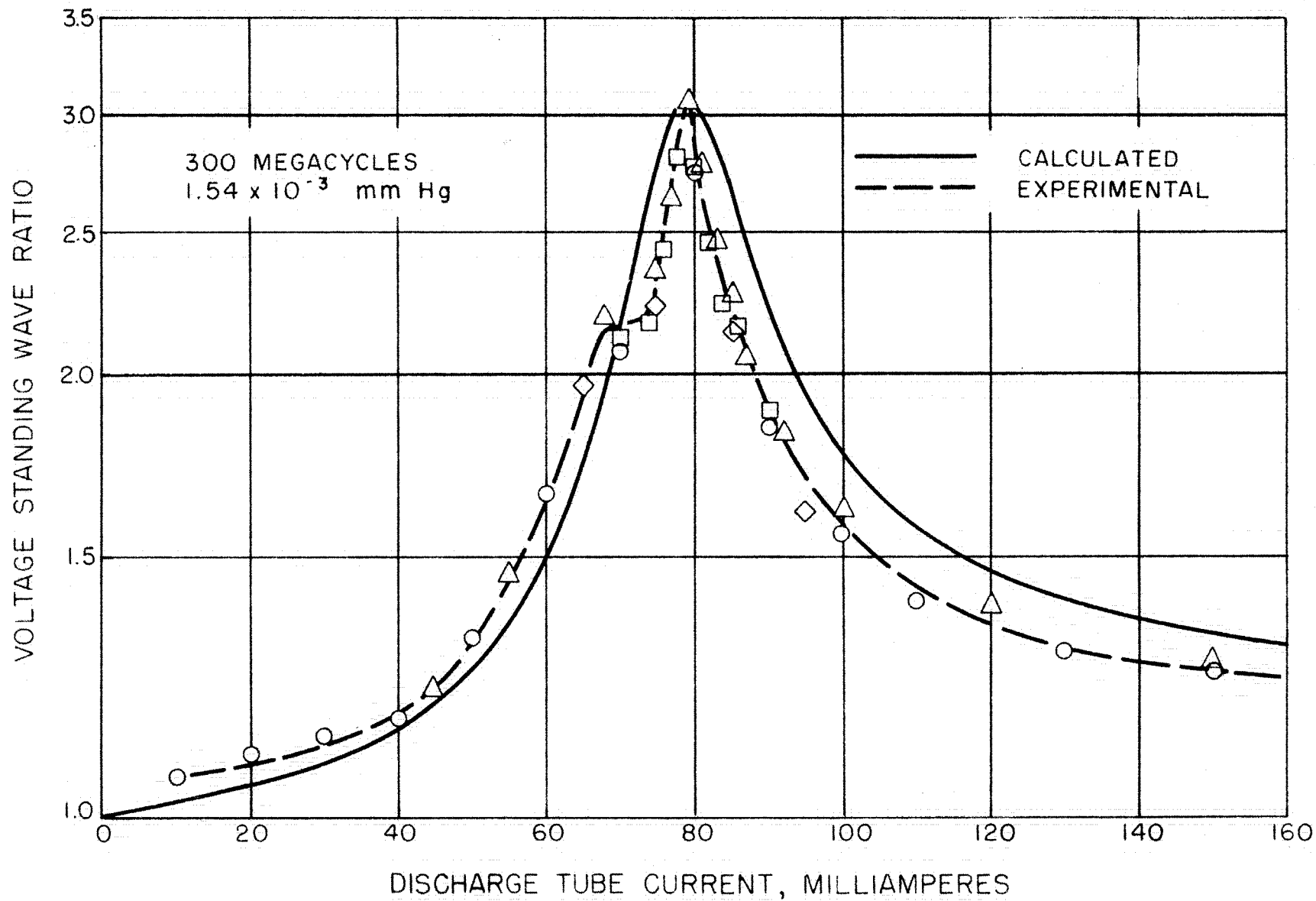


Figure.7. Standing Wave Ratio versus Discharge Current

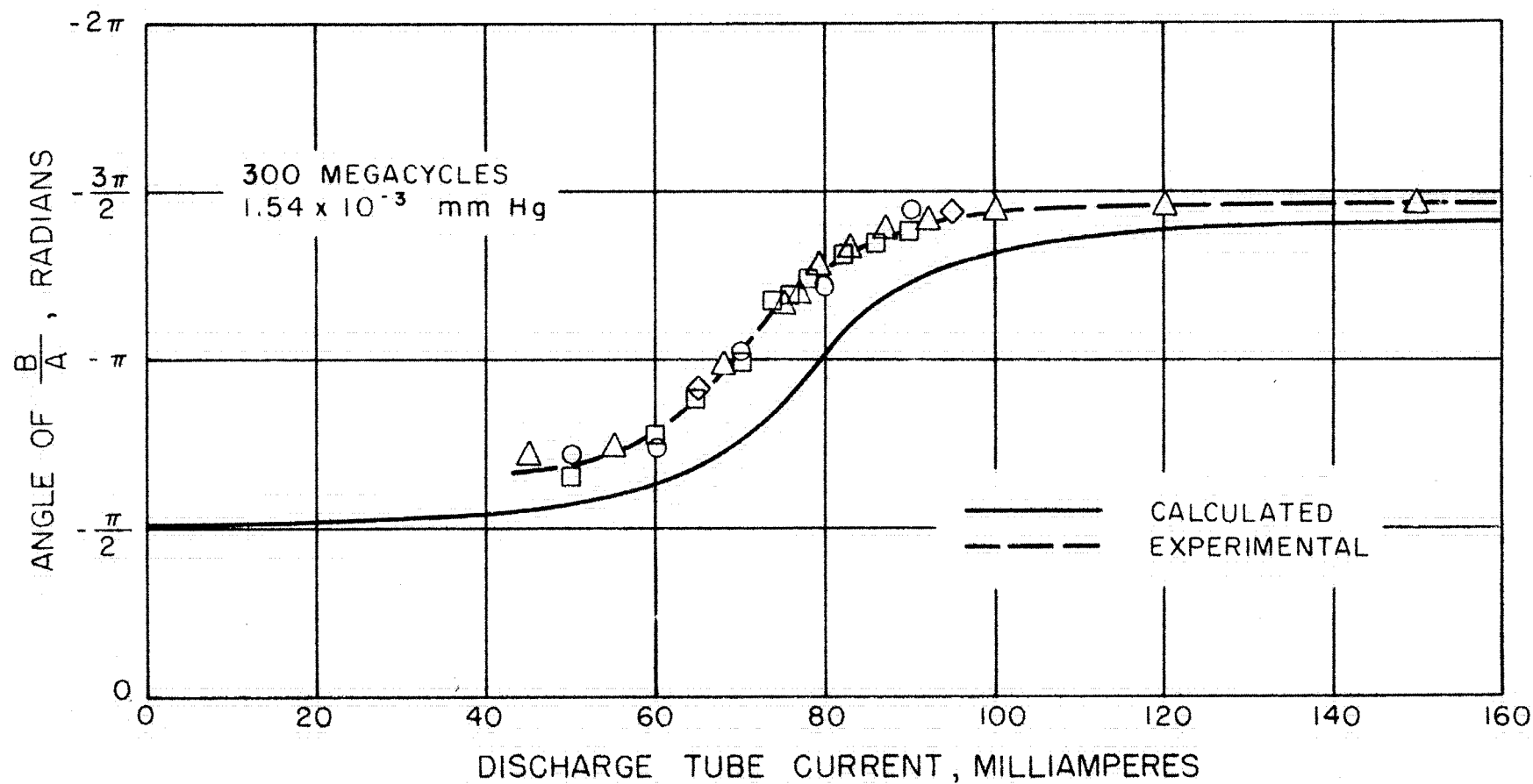


Figure 8. Angle of B/A is Discharge Current

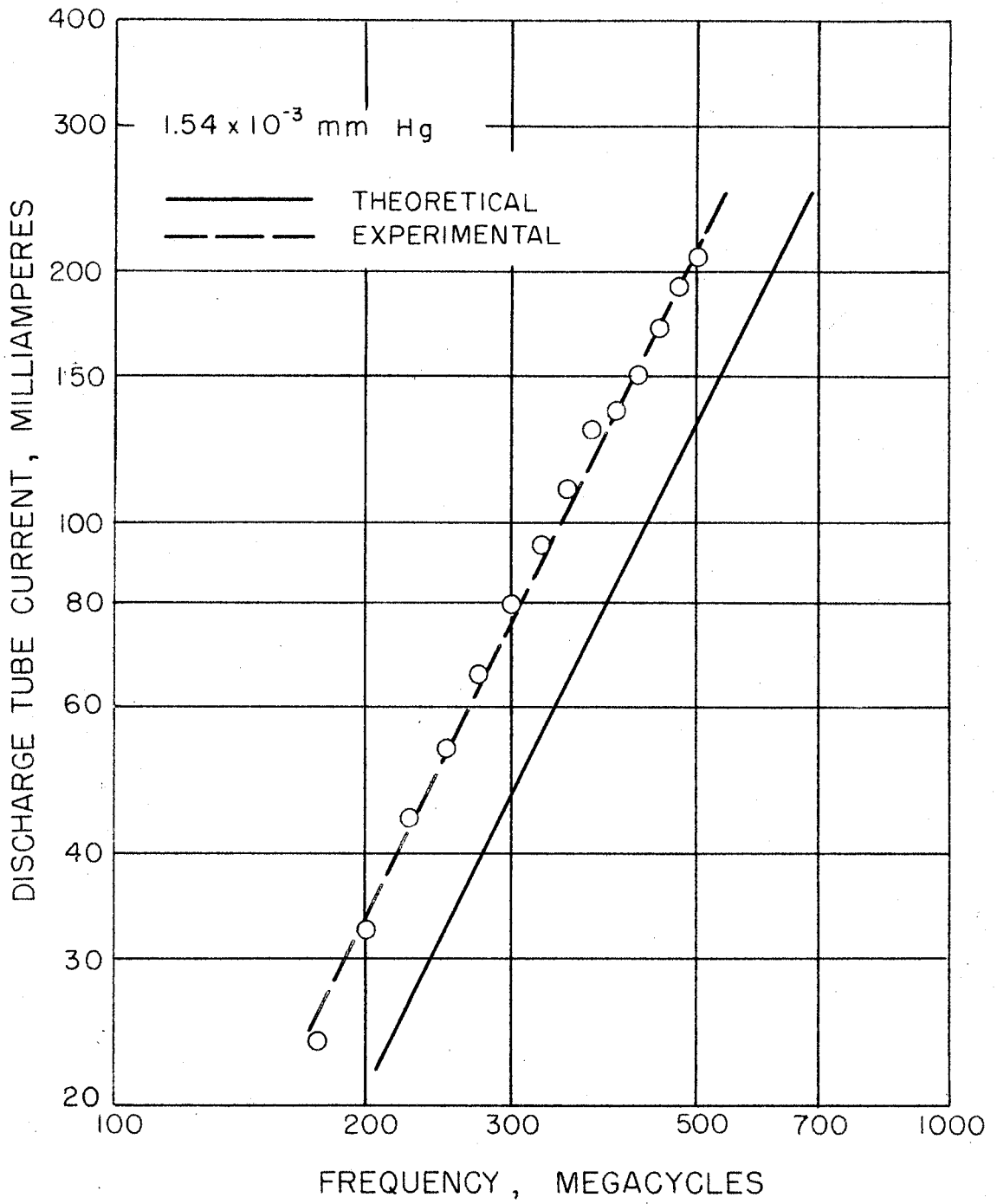


Figure 9. Current for Resonance vs. Frequency

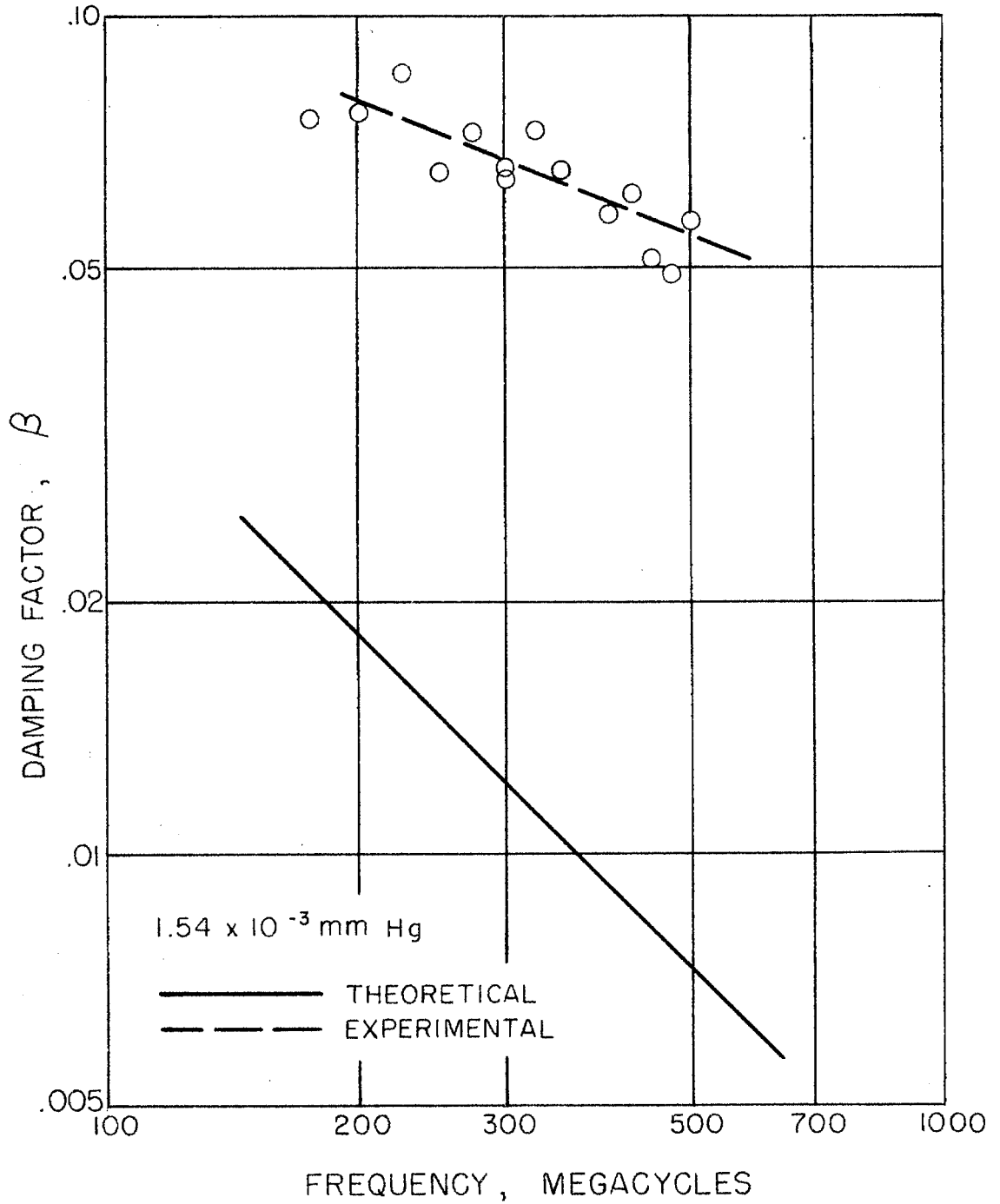


Figure 10.  $\beta$  versus Frequency



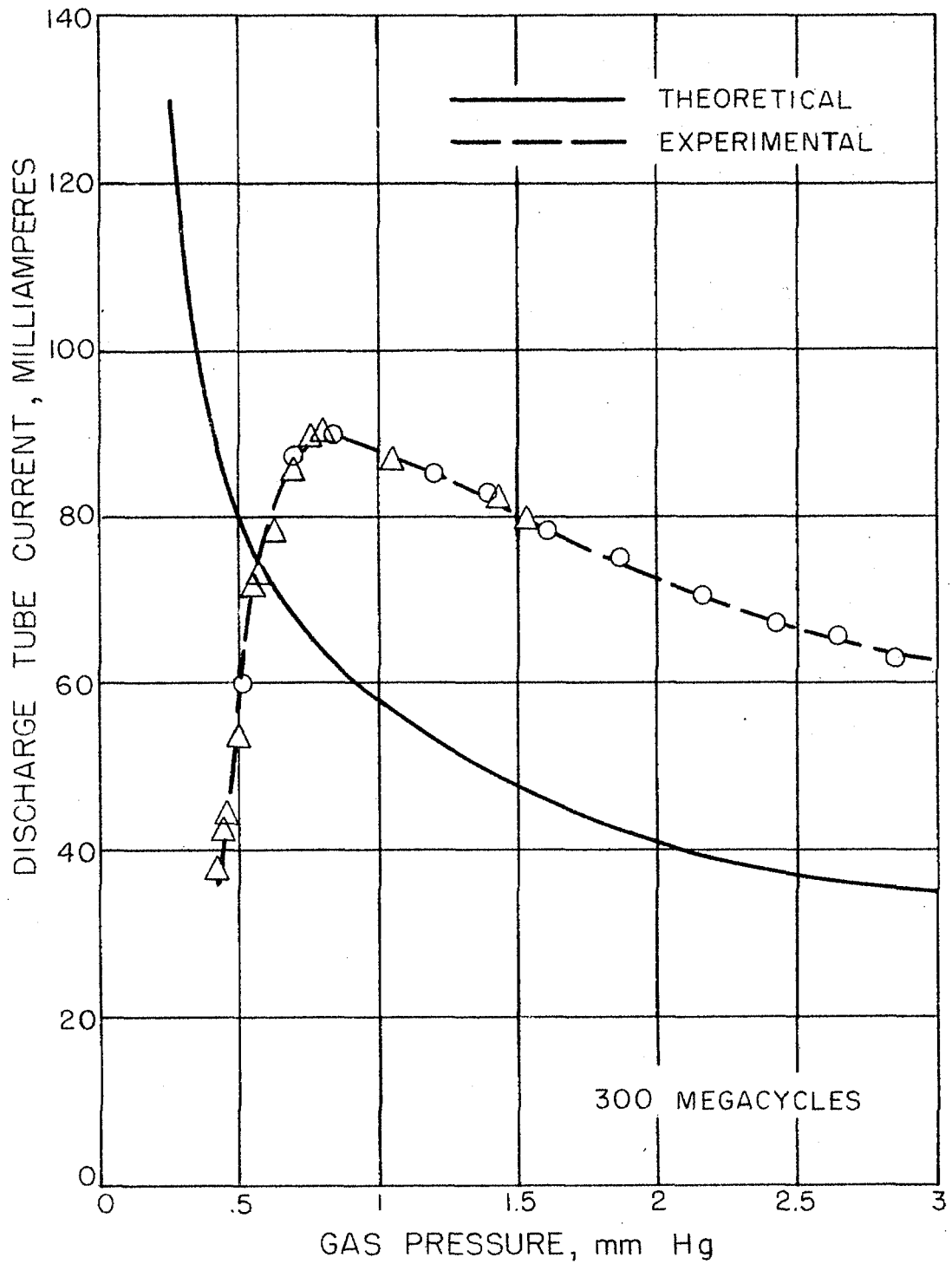


Figure 11. Current for Resonance vs. Gas Pressure

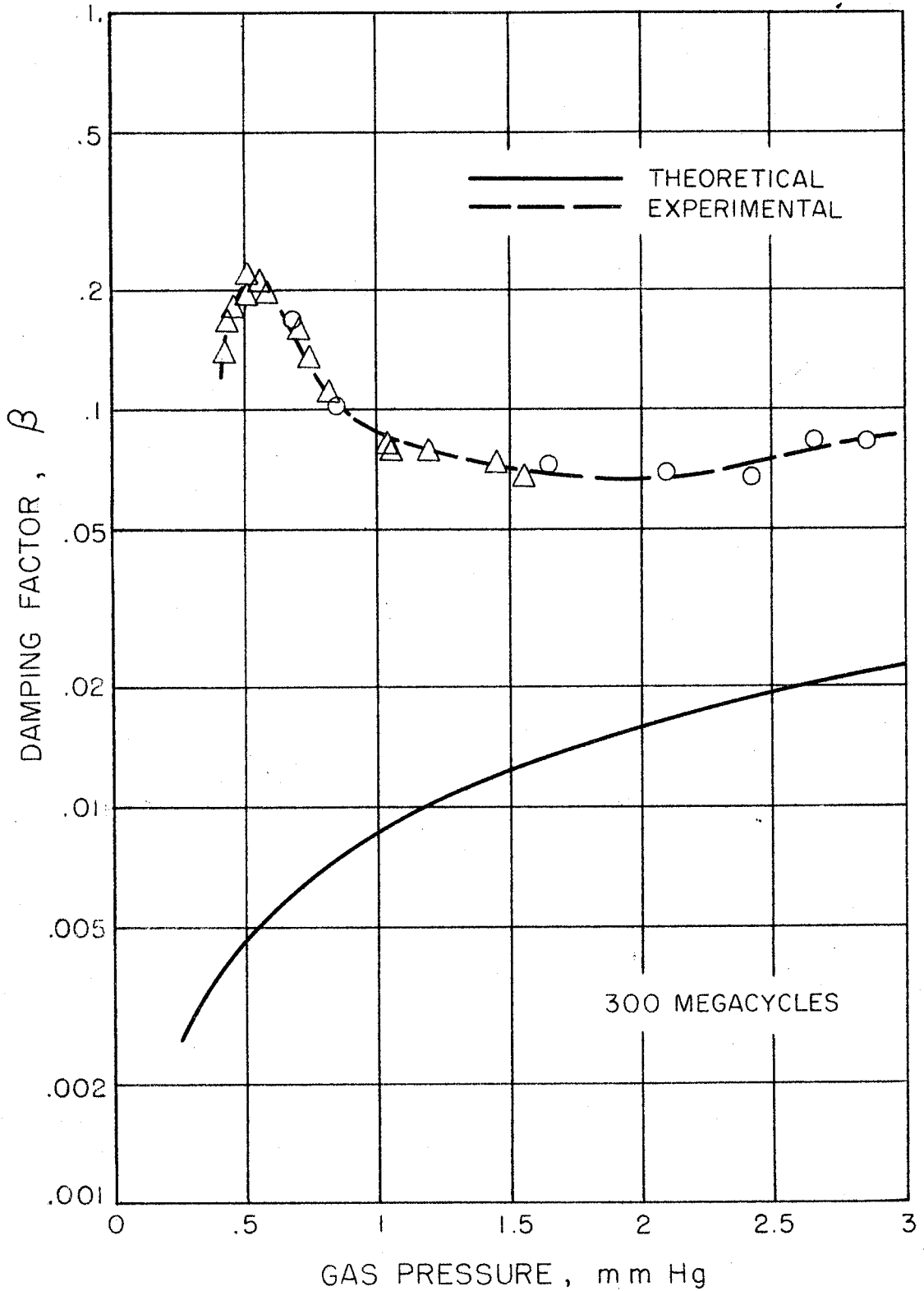


Figure 12.  $\beta$  versus Gas Pressure

VI LIST OF REFERENCES

1. Bullington, K.  
Characteristics of Beyond the Horizon Radio Transmission  
Proceedings of the IRE, V.43 (1955) pp. 1175-1180.
2. Herlofson, N.  
Plasma Resonance in Ionospheric Irregularities  
Arkiv För Fysik, V.3 (1951) pp. 247-297.
3. Kaiser, T. R. and Closs, R. L.  
Theory of Radio Reflections from Meteor Trails  
Philosophical Magazine, V.43, 7th Series, (1952), pp. 1-32.
4. Lovell, A. C. B.  
Meteor Astronomy (book) pp. 23-85  
Clarendon Press, Oxford, (1954)
5. Eckersley, T. L.  
Transmission of Electric Wave through the Ionized Medium  
Philosophical Magazine, V.4, 7th Series (1927), pp. 147-165.
6. Tonks, L.  
High Frequency Behavior of a Plasma  
Physical Review, V.37 (1931), pp. 1458-1483.
7. Tonks, L.  
Plasma-Electron Resonance, Plasma Resonance, and Plasma Shape  
Physical Review, V.38 (1931), pp. 1219-1223.
8. Romell, D.  
Radio Reflexions from an Ionized Column of Gas  
Nature, V.167 (1951), p. 243.
9. Margenau, H.  
Conduction and Dispersion of Ionized Gases at High Frequencies  
Physical Review, V.69 (1946), pp. 508-513.

10. Adler, F. P. and Margenau, H.  
Electron Conductivity and Mean Free Paths  
Physical Review, V.79 (1950), pp. 970-971.
11. Everhart, E. and Brown, S. C.  
The Admittance of High Frequency Gas Discharges  
Physical Review, V.76 (1949), pp. 839-842.
12. Allis, W. P; Brown, S.C. and Everhart, E.  
Electron Density Distribution in a High Frequency Discharge in  
the Presence of Plasma Resonance  
Physical Review, V.84 (1951), pp. 519-522.
13. Adler, F. P.  
Measurement of the Complex Conductivity of an Ionized Gas at  
Microwave Frequencies  
Journal of Applied Physics, V.20 (1949), pp. 1125-1129.
14. Eccles, W. H.  
On the Decimal Variations of the Electric Waves Occurring in  
Nature, and on the Propagation of Electric Waves Round the Bend  
of the Earth  
Proceeding of the Royal Society of London, Series A, V.87, (1912),  
pp. 79-99.
15. Smythe, W. R.  
Static and Dynamic Electricity (book)  
McGraw Hill Book Company, Second Edition (1950)
16. Mackinson, R. E. B. and Slade, D. M.  
Dipole Resonant Modes of an Ionized Gas Column  
Australian Journal of Physics, V.7 (1954), pp. 268-278.
17. Keitel, G. H.  
ON the Dipole Resonant Mode of an Ionized Gas Column  
Australian Journal of Physics, V.9 (1956), pp. 144-147.

18. Keitel, G. H.  
Certain Mode Solutions of Forward Scattering by Meteor Trails  
Proceedings of the IRE, V.43 (1955), pp. 1481-1487.
19. Howe, R. M.  
Probe Studies of Energy Distributions and Radial Potential Variations in a Low Pressure Mercury Arc  
Journal of Applied Physics, V.24 (1953), pp. 881-894.
20. Dwight, H. B.  
Tables of Integrals and Other Mathematical Data (book)  
The Macmillan Company, New York (1934)
21. Klarfeld, B.  
Characteristics of the Positive Column of a Gaseous Discharge  
Journal of Physics of the USSR, V.5 (1941), pp. 155-175.
22. Brode, Robert B.  
The Absorption Coefficient for Slow Electrons  
Physical Review, V.35 (1930), pp. 504-508.
23. Killian, Thomas J.  
The Uniform Positive Column of an Electric Discharge in Mercury Vapor  
Physical Review, V.35 (1930), pp. 1238-1252.